Università
Ca'Foscari
Venezia

Master's Degree Programme in
Conservation Science and Technology for
Cultural Heritage
ex D.M. 270/2004

Final Thesis

Characterization and monitoring over time of oil-based pictorial products manufactured by the Belgian company Jacques Blockx and their use in the 20th century painting *The temptation of Saint Anthony* by Salvador Dalí

Graduand
Daniela Aleccia
Matriculation Number 867814

Supervisor
Prof. Francesca Caterina Izzo

Assistant supervisors
Prof. David Strivay
Prof. Catherine Defeyt
Dr. Margherita Gnemmi

Academic Year
2022-2023

Contents

Aim of the thesis

Since 1865, Blockx artists' paints manufacture (Belgium) has been widely used by artists all over the world for its quality oil paints. Among these artists stands Salvador Dali (1904-1989), as the Spanish painter himself states in his book "50 Secrets of Magical Craftsmanship" (1948) [1]. Starting from this important reference, the aim of this thesis is to characterize and study the oil painting products purchased by the Belgian company over time and to possibly relate them to the materials used by the artist Salvador Dalí.

This project was developed by the University of Liège, in particular by the Centre Européen d'Archéométrie (CEA), and then carried out in collaboration with Ca' Foscari University of Venice thanks to an Erasmus+ internship. The CEA is involved in the *Face to Face* project of the Royal Museums of Fine Arts of Belgium, whose aim is to shed new light on the representation of human faces in Western painting through the prism of technical art history.

To this purpose, in 2019 a first analytical campaign on the painting "The temptation of Saint Anthony" by Salvador Dalí (dated 1946 - Royal Museum of Fine Arts of Belgium in Brussels) was carried out. In 2020 a second research was conducted thanks to the master thesis "Analyse par spectroscopies vibrationnelles et fluorescence des rayons X de l'œuvre « La Tentation de Saint-Antoine » de Salvador Dalí" by Soline Hardy, tutored by prof. David Strivay and prof. Catherine Defeyt [2].

Based on the results of the previous studies, the present thesis aims to investigate the relationship between the Belgian company and the Spanish painter through a physico-chemical study. The first phase of the research consisted of the preparation of a uniform set of samples made with selected Blockx commercial oil paints. In particular, the products available for this study were eight tubes of oil paints and three amber-based painting solutions currently sold by Blockx. Among the oil paints, three of them are recent, from 2010, and the other five are considered "historical", from the 20th century. A multi-analytical approach was adopted to gather information on the composition and film-forming processes of the mock-ups made using attenuated total reflection infrared spectroscopy (ATR-FTIR), gas chromatography-mass spectrometry (GC-MS) and weight percentage variation calculation.
The second phase of this research consisted of the study of Salvador Dalí painting "The temptation of Saint Anthony" that was performed using energy dispersive X-ray fluorescence

(EDXRF), Micro-Raman spectroscopy, ATR-FTIR, scanning electron microscopy with energy dispersive X-ray spectroscopy (SEM-EDX) and GC-MS.

Objectifs du mémoire

Depuis 1865, la manufacture de peintures d'artistes Blockx (Belgique) est largement utilisée par les artistes du monde entier pour ses peintures à l'huile de qualité. Parmi ces artistes figure Salvador Dali (1904-1989), comme le peintre espagnol l'indique lui-même dans son livre "50 Secrets of Magical Craftsmanship" (1948) [1]. À partir de cette référence importante, l'objectif de cette thèse est de caractériser et d'étudier les produits de peinture à l'huile achetés par l'entreprise belge au fil du temps et de les mettre éventuellement en relation avec les matériaux utilisés par l'artiste Salvador Dalí.

Ce projet a été développé par l'Université de Liège, en particulier par le Centre Européen d'Archéométrie (CEA), puis réalisé en collaboration avec l'Université Ca' Foscari de Venise grâce à un stage Erasmus+. Le CEA est impliqué dans le projet Face to Face des Musées royaux des Beaux-Arts de Belgique, dont l'objectif est d'apporter un éclairage nouveau sur la représentation des visages humains dans la peinture occidentale à travers le prisme de l'histoire de l'art technique.

À cet effet, en 2019, une première campagne d'analyse sur le tableau "La tentation de saint Antoine" de Salvador Dalí (daté de 1946 - Musée royal des beaux-arts de Belgique, Bruxelles) a été menée. En 2020, une seconde recherche a été conduite grâce au mémoire de master "Analyse par spectroscopies vibrationnelles et fluorescence des rayons X de l'œuvre "La Tentation de Saint-Antoine" de Salvador Dalí" de Soline Hardy, encadrée par les prof.rs David Strivay et Catherine Defeyt [2].

Sur la base des résultats des études précédentes, la présente thèse vise à étudier la relation entre l'entreprise belge et le peintre espagnol par le biais d'une étude physico-chimique. La première phase de la recherche a consisté en la préparation d'un ensemble uniforme d'échantillons réalisés avec des peintures à l'huile commerciales Blockx sélectionnées. En particulier, les produits disponibles pour cette étude étaient huit tubes de peinture à l'huile et trois solutions de peinture à base d'ambre actuellement vendus par Blockx. Parmi les peintures à l'huile, trois sont récentes, datant de 2010, et les cinq autres sont considérées comme "historiques", datant du 20e siècle. Une approche multi-analytique a été adoptée pour recueillir des informations sur la composition et les processus de formation du film des maquettes réalisées à l'aide de la spectroscopie infrarouge à réflexion totale atténuée (ATR-FTIR), de la chromatographie gazeuse-spectrométrie de masse (GC-MS) et du calcul de la variation du pourcentage de poids.

La deuxième phase de cette recherche a consisté en l'étude du tableau de Salvador Dalí "La tentation de Saint Antoine", qui a été réalisée à l'aide de la fluorescence de rayons X à dispersion d'énergie (EDXRF), de la spectroscopie Micro-Raman, de l'ATR-FTIR, de la microscopie électronique à balayage avec spectroscopie X à dispersion d'énergie (SEM-EDX) et de la GC-MS.

1. Introduction

1.1. Oil binding medium in paintings

In the history of painting, oil has been the dominant paint medium all over the world for over five hundred years since the 15th century. The invention of oil painting technique was commonly attributed to the Flemish artist Jan van Eyck (1390-1441), as reported by Giorgio Vasari in his treatise *Le vite* [3]. Recent studies even attest that the earliest known examples of oil painting date back to 7th century [3, 4]. These are cave paintings (murals), depicting images of Buddhas, bodhisattvas, and female devotees, discovered in 2008 in the historic village of Bamiyan in Afghanistan, a former site on the silk trade route. They have been found in a good conservation state and their refinement suggested that the oil medium was already used in Asia for some time. Though van Eyck cannot be credited as the inventor of oil painting, it is possible to affirm that his innovative use of the medium has inspired many other artists of the time and has helped to popularize this painting technique throughout Northern Europe and then in Italy. Indeed, Jan van Eyck developed a technique defined as a new and prodigious manner of coloring by Vasari, which consisted of the application of multiple transparent glazes of oil paint on egg tempera underpainting, allowing for great intensity and depth of color [6]. This technique would later be perfected in Italy by artists such as Giorgione (1478-1510) and Tiziano (1490-1576) during the Italian Renaissance. The latter was the first to experiment with painting made exclusively in oil because it allowed for a more transparent and less opaque paint. Since then, oil painting technology underwent only slight modifications, thus remaining the most widely used painting method among artists.

1.1.1. From traditional to commercial oil paints (20th century)

Oils used as binding medium are vegetable oils, but just the ones which are able to form a dry film when exposed to air. The most common drying oils used since medieval times are linseed, poppyseed and walnut oil [7]. These oils are extracted from vegetable seeds and respectively from flax *Linum usitatissimum*, from the seeds of *Papaver somniferum* and the latter from the walnuts [8]. According to the traditional technology, to obtain the oil from the seeds or the flax plant the pressure method has been always used. Then in the modern oil production this method was coupled with solvent extraction to increase the yield of oil [7]. The main steps consisted of cleaning the seeds, separating them from other materials like chaff etc. and removing particles of other sizes, and then grinding them to a fine meal to make easier the oil extraction.

The final process was the so called *cooking* and it consisted of heating the meal before pressing it to extract the oil [7]. Then to make oil paint, the oil medium was mixed with pigments accurately grinded by the artists themselves and with other few ingredients for example essence of turpentine, a vegetable solvent used to dilute oil colours and to decrease viscosity or litharge (lead oxide) to increase the siccative properties of oil, a technique introduced by Antonello da Messina (1430-1479) [8].

The traditional oil paint technology lasted until around the 18th century, before a great technical and formal revolution which started from the Industrial Revolution and further developments in the late 19th century. Then the paint technology developed slowly during the first two decades of the 20th century, probably catalyzed by the two world wars [9].

If until the 18th century the entire production of oil paints was carried out by artists in their ateliers according to personal and sometimes secret recipes, from the 19th century the production of oil paints became more and more industrial essentially responding to a distinct demand by artists. Indeed, these changes coincided with the development of painting techniques other than the traditional ones, such as the *en plein air* painting performed by the Impressionists [10]. A significant innovation of this period is in fact the first collapsible tin tube introduced for the first time in the art market by the British company Winsor & Newton in 1841 which allowed to paint also outside the artists' studios [11].

Oil paints thus became commercial products, so their formulations underwent considerable changes, at the expense of their quality, which is inferior to the artistic formulations historically used in the art world. As mentioned above, before modern paint tubes and thus, the production of a proper range of fine art oil paints, artists made their own oil paints. Indeed, an essential part of their art training was to know the properties of pigments, their compatibility with other pigments, their stability, the drying attributes etc [12]. Instead from 19th century paint manufactures started to produce oil paints on an larger scale, so formulations included several additives which enable faster production, stability, right consistency, extended shelf life and sometimes also fillers and adulterants to offer more affordable products [8]. It is also essential to consider the introduction of other oils in addition to the most common drying ones, such as other drying oils or semi-drying and non-drying ones due to their low cost and easy availability compared to poppyseed and walnut oil [13]. Since the 20th century safflower, sunflower, castor, and cotton-seed oils have been commonly employed. They exhibited different characteristics and behaviour, such as a certain slowness in the drying process and in the formation of the pictorial film which forced manufactures to add other ingredients to increase performances e.g.,

driers, or to pre-treat oils by heating them or heating them in absence of oxygen (producing Stand oil) or even by formulating acid or alkaline refining [11].

In general, the main additives used in commercial paint formulations are stabilizers, driers (or siccatives), dispersion agents (or wetting agents), whiteners, extenders, fillers, and adulterants.

- Stabilizers are components mainly used to keep the pigments in suspension and give the desire consistency to the paint. They can be waxes or wax-materials such as hydrogenated castor oil known also as castor wax (added up to 2%/w), water or water solutions, and inert pigments like alumina hydrate. It is possible to find also free fatty acids [11].
- Driers are used to accelerate the drying process and thus the pictorial film formation. Traditionally lead-based pigments like lead white, litharge, or minium were added because it was known that they acted like catalyst for the polymerization reactions of oil medium [14]. Today cobalt- and zinc-based pigments are commonly used. These metal salts are added for less than 0.1% to maintain a good quality of paint.
- Dispersion agents are used to improve the dispersion of the pigment in the medium and the paint's working properties increasing the viscosity [15]. Typically, metal stearates (or soaps) are used e.g., aluminum, zinc, and magnesium stearates for fast wetting, but also as a gelling agent. It is added a maximum of 2% of stearate because an excess of it can cause rigidity of paint films [8]. Also pigments such as zinc oxide can be added to the formulation because they are able to form metal soaps over time.
- Extenders and fillers are white inorganic minerals mainly used to increase the amount of product and thus lower the prices . The fillers commonly used are silica, clay, calcium carbonate, magnesium carbonate, aluminum silicate, silica, hydrated magnesium silicate (talc), barium sulphate, and calcium sulphate dihydrate. These minerals have refractive indices similar to that of the binder and they can include color impurities [9]. Unlike fillers, extenders are also used to improve the consistency and rheological properties of the paint [16].
- Whiteners are used to make white pigments appear brighter and opaquer. Titanium white is used with other white pigments such as calcium carbonate, calcium sulphate dihydrate and barium sulphate.

1.1.2. The chemical composition of drying oils

Drying oils used in paintings are mainly composed of triacyglycerols (TAGs) or triglycerides which are triesters of glycerol (1,2,3-propanatriol) and a mixture of linear long-chain fatty acids which can be saturated or unsaturated [7]. The variety of the fatty acids found in oils after

hydrolysis is very large indeed triglycerides can be arranged in more than forty possible ways [8]. However, the fatty acids most commonly found in drying oils are limited in number and they are listed and described in **Table 1** with their relative degree of unsaturation and their melting point. Drying oils are mainly composed of saturated acids like lauric (C12), myristic (C14), palmitic (C16) and stearic (C18) acids, and C18 polyunsaturated acids with one, two or three double bonds (oleic, linoleic and linolenic acids, respectively) [17].

The proportions and types of fatty acids forming the triglyceride molecules are directly responsible for the chemical and physical properties of the oil, such as its melting point and drying power. Indeed, according to the table drying oils which have a high concentration of shorter saturated fatty acids (C9-C14) and longer unsaturated fatty acids (C18:1, C18:2, C18:3 in cis configuration) are liquid at room temperature with a melting point below 25 °C.

Table 1 The main saturated and unsaturated fatty acids present in drying oils [18].

Common name	IUPAC name	Formula	Abbreviation	Melting point (°C)
Lauric	Dodecanoic	$C_{12}H_{24}O_2$	C12	44
Myristic	Tetradecanoic	$C_{14}H_{28}O_2$	C14	54
Palmitic	Esadecanoic	$C_{16}H_{32}O_2$	C16	63
Palmitoleic	9-Esadecanoic	$C_{16}H_{30}O_2$	C16:1	0.5
Stearic	Octadecanoic	$C_{18}H_{36}O_2$	C18	70
Oleic	9-Octadecanoic	$C_{18}H_{34}O_2$	C18:1	16
Linoleic	9,12-Octadecadienoic	$C_{18}H_{32}O_2$	C18:2	-5
Linolenic	9,12,15- Octadecatrienoic	$C_{18}H_{30}O_2$	C18:3	-11
α-aleostearic	Cis,trans,trans-9,11,13-Octadecatrienoic	$C_{18}H_{30}O_2$	α-C18:3	49
Ricinoleic	12-hydroxy-9-octadecanoic	$C_{18}H_{34}O_2$	-	-

Moreover, the drying power of an oil is related to the presence of oleic, linoleic and linolenic acids which are called C18 non-conjugated unsaturated fatty acids because they present double bonds interspersed with single methylene groups [7]. The reactivity is due to the double bonds that react with the oxygen of air and with another fatty acid forming the polymeric film [17]. Oils are thus classified as drying oil, semi-drying oil and non-drying oil based on the ability or inability to form solid films by exposing to air. In **Table 2**, the range of fatty acid compositions of the three most common drying oils used in the history of painting are shown. It is known that linseed oil has better performances if compared with poppyseed and walnut oil; that is because of its faster drying due to a higher amount of linolenic acid, which is the most unsaturated fatty acid that can be present in a drying oil [18]. In addition to the TAGs, linseed oil as well as other siccative oils is also composed of smaller amounts of other compounds: 0.5-2% of free fatty acids both saturated and unsaturated, such as arachidic acid (C20), behenic

acid (C22), lignoceric acid (C24), palmitoleic acid (C16:1) and arachidoic acid (C20:1); 0.1-2% of water dissolved in oil; phosphatides and mucilaginous materials like lecithin (up to about 1%) which is a phospholipid with an emulsifying function [7]. Furthermore, in addition to the lipid part, fresh oils contain a non-saponifiable fraction (1-3%) which consists of coloring materials such as beta-carotene or chlorophyl whose oxidation cause the oil to brown, and different sterols (0.2-0.4% phytosterols in linseed oil). Other components present in trace are paraffins (0.01-01%), waxes, triterpenic alcohol like squalene (0.15%) and tocopherols (around 0.1%). Tocopherols are antioxidants and they protect naturally vegetable oil from oxidation. Nevertheless, the presence of these kind of constituents cause a delay in the drying process, called induction period, which influence an important aspect of a drying oil used in art [19].

Table 2 Percentage of five major fatty acids present in linseed, poppyseed and walnut oil [7], [18].

OIL	Fatty acid (% of total fatty acids)				
	Palmitic	**Stearic**	**Oleic**	**Linoleic**	**Linolenic**
Linseed	4-10	2-8	10-24	12-19	48-60
Poppyseed	9-11	1-2	11-18	69-77	3-5
Walnut	3-8	0.5-3	9-30	57-76	2-16

Drying oils can be processed to improve their properties. They are usually treated to increase the viscosity (pre-polymerization) and to modify the drying time by introducing chemical changes into the oil composition. Two main methods have been always applied, which are simple heating and air blowing [7]. For example, stand oil is one of the most famous processed oil which historically was made by exposing flaxseed to sunlight for long periods of time in a glass jars [20]. Now this pre-polymerized linseed oil is produced by heating it at 210-310 °C in the absence of oxygen. This process causes the oil to partially polymerize across the carbon-carbon double bonds resulting in a paler and thicker and more viscous oil which is slow drying but has great stability and durability properties [19].

1.1.3. The drying mechanism of drying oils

Drying oils have been historically exploited in the artistic techniques because of their ability to dry and form a polymeric film of hard and resinous consistency with excellent mechanical and optical properties which is called paint film [21]. The drying or siccative process is a complex reaction called oxidative polymerization in which several factors play an important role. In general, the siccative property is linked to the presence of unsaturated fatty acids (UFAs) in the oil composition. Indeed, the most important chemical reaction of the curing and ageing of the oil is the spontaneous reaction between the oxygen and the UFAs. Oils are thus classified as

drying oil only if the amount of UFAs is at least 66% of the total fatty acids. When the percentage of UFAs is lower than 66% oils can be classified as semi-drying when they form sticky films as cottonseed oil or non-drying oils when they remain fluid in air as castor oil [7]. Both linoleic and linolenic acids contribute to the degree of unsaturation; for example, linseed oil is composed of 20% of linoleic acid and 50% of linolenic acid, as it is reported in Table 2. In the case of non-conjugated oils, i.e., those whose double bonds are not separated by methylene groups, the drying index (D.I.) is very useful to assess the siccativity and it must be greater than 70% for drying oils [7]. It expressed as follows:

$$D.I. = (\%\ linoleic\ acid) + 2\ (\%\ linolenic\ acid).$$

Basically, the curing of drying oils consists of a two-phase process: initial uptake of atmospheric oxygen by the carbon-carbon double bonds within the UFAs (autoxidation), followed by decomposition of the oxidation products, which initiates cross-linking and therefore the formation of the paint film itself (oxidative polymerization).

These reactions can all occur simultaneously but typically the curing of oils is preceded by the induction period which can last few hours, as mentioned before (par. 1.1.2). In this phase tocopherols present in the oil composition act as anti-oxidising by inhibiting the drying process [21].

Then the autoxidation occurs when the atmospheric oxygen (triplet oxygen, $^3O_2$) absorbed by the oil film spontaneously starts to react with the UFAs present in the oil producing active radical species [7]. This is an autocatalytic reaction in which the oxygen acts as a radical initiator, thus its rate increases with the progression of the drying process. For example, linseed oil spread in thin films absorbs initially slowly, then more rapidly, significant amounts of oxygen, approximately 20-30% of its weight [14].

The first step of autoxidation (initiation) consists of the subtraction of a hydrogen from a methylene group -CH_2 (RH) by the radical initiator ($In^{\bullet}$) forming free radicals ($R^{\bullet}$) and occurs preferentially on the allyl CH_2 between two double bonds.

$$In^{\bullet} + RH \rightarrow R^{\bullet} + InH \quad (1)$$

Subsequently, the carbon radicals formed tends to be stabilized through various resonance structures and by a molecular rearrangement leading to the formation of conjugated dienes (as shown in **Figure 1**).

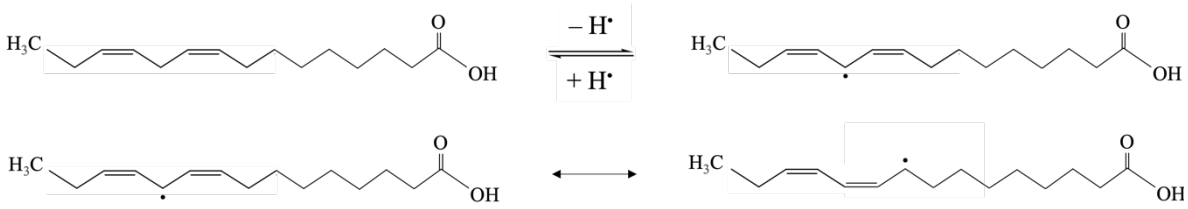

Figure 1 Representation of the molecular rearrangement and resonance stabilization of an UFA after the initiation step of autoxidation.

The resulting dienes start the propagation phase when the carbon radicals combine with atmospheric oxygen to generate peroxide (ROO•) radicals, according to the following reaction:

$$R^{\bullet} + O_2 \rightarrow ROO^{\bullet} \quad (2)$$

Without the presence of catalyzers, this reaction can occur in 2-3 days [14] and it is possible to observe a significant change of some chemical-physical properties of the oil such as an increase in viscosity and a change in the refractive index.

The peroxide radicals are then able to extract a hydrogen atom from adjacent lipid molecules to give hydroperoxides (3) which then decompose into alkoxy and hydroxyl radicals (4).

$$ROO^{\bullet} + RH \rightarrow ROOH + R^{\bullet} \quad (3)$$

$$ROOH \rightarrow RO^{\bullet} + {}^{\bullet}OH \quad (4)$$

All these highly reactive compounds generated during the propagation step trigger the second phase of the curing process, called oxidative polymerization. This phase leads to the formation of intermolecular bonds between different triglycerides present in the oil film until, gradually, a three-dimensional cross-linked molecular structure is built up [7]. Within this structure may remain unoxidized triglycerides which are in liquid state; these fractions present in structural voids flex the film giving it strength, cohesion, and elasticity, which are fundamental characteristics for a good drying oil used in art.

The oxidative polymerization may occur by the radicals bimolecular recombination during the termination step of autoxidation, or by the reaction between the formed radicals (peroxide (ROO•) and alkoxy (RO•) ones) and the double bonds of the unsaturated fatty acids still present in the oil forming new peroxidic (ROOR) or etheric (ROR) bridges bonds between triglycerides and free fatty acids [17]. In the first case, the most likely recombination is that of two peroxide radicals giving an intermediate tetroxide, but other rearrangements occur forming mainly dimers of TAGs. Nevertheless, almost all TAGs in drying oils present multiple unsaturated fatty acids, so oxygen can be incorporated on multiple positions. As a result, higher oligomers are formed and this increases the average molecular weight and thus the viscosity of the oil [7].

In this way the oil film dries, and an insoluble polymer is formed. However, the process of cross-linking continues for a long time after the paint film has dried, eventually causing the paint film to become brittle, crack, and disintegrate [18]; phenomena that will be discussed in the following paragraph. For example, a film of linseed oil becomes dry to the touch within a few days, but the curing process continues for many years, and thus the hardening, until all the polyunsaturated bonds in TAGs disappear [17], [22].

The phenomenon that indicates the occurrence of reactions within the oil film is the weight change of the film itself. It is known that an oil film will gain weight (about 20%, depending on the number of double bonds present in the oil) after the induction period due to the uptake of atmospheric oxygen and thus the polymerization and then it will undergo a mass loss caused by the evaporation of volatile organic compounds (VOCs) formed with progressive ageing [23]. Indeed, during the oxidative polymerization and thus the formation of high molecular weight material also several low-molecular weight compounds called VOCs are formed by the fragmentations of the oxidation products of triglycerides, and this process continues for the entire lifetime of the film [24]. Generally, weight loss begins to level off after about one year and, after two years, even if the weight loss continues there are only small differences.

These volatile fragments are mainly aldehydes, ketones, alcohols, but also alkyl, and vinyl radicals which can react with other radicals such as $H^{\bullet}$ and $OH^{\bullet}$ producing respectively aldehydes or hydrocarbons [7]. These are secondary oxidation products whose evaporation together with the water present in the oil matrix can be easily detected by the typical acrid smell of drying oil.

Different reactions contribute to the formation of these secondary products. In particular, alkoxy radicals ($RO^{\bullet}$) formed by homolytic cleavage of hydroperoxides (4) undergo a decomposition by β scission of adjacent C-C and C-H bonds forming an aldehyde and an alkyl radical which may react with oxygen and produce an aldehyde [17].

Finally, the tertiary oxidation products are generated by oxidative cleavage of the secondary ones, peroxides radicals, or hydroxyl radicals. These are dicarboxylic acids (diacids), dihydroxy acids and hydroxylated monocarboxylic acids [8]. Among them, the most abundant compound is azelaic acid which is the result of the oxidative cleavage of the double bond at the C9 position of unsaturated fatty acids with eighteen atoms of carbon (oleic, linoleic, and linolenic acids) [23]. Other products are diacids like suberic and sebacic acids, with eight and ten atom of carbons respectively, small amounts of monocarboxylic acids, and other components including epoxy-, oxo-, and hydroxyl- by-products [7]. In particular, the dicarboxylic acids are relatively stable, and they can be considered end-products of the drying

process. Their presence is normally attested in dried oil films testifying the original abundance of unsaturated fatty acids in the oil composition [8].

1.1.4. Degradation of oil paintings

When the oil film dries, it forms an elastic and insoluble polymer, called linoxyn in the case of linseed oil. However, this film tends to become fragile and brittle as the oil ages over time, due to a degradation process that may already start during the oil film curing, resulting in a cracked layer and sometimes also with powdery consistency. This degradation happens because of the fragmentation of the polymeric structure due to oxidative and hydrolytic processes that may occur over time and the consequent formation of hydrophilic compounds, such as carboxylates and hydroxylate, that contribute to water penetration into the matrix, although the film was originally hydrophobic and apolar [8]. The absorption of water turns to be very dangerous for the oil paint because it leads to partial hydrolysis of ester bonds of TAGs causing the releasing free fatty acids. This causes a weakening of the paint film itself and other mechanical issues like swelling, shrinkage, loss of adhesion or delamination.

In addition to water sensitivity which can be also related to phase separation of components in the original paint formulations [15], the degradation of oil films can cause also other stability issues including color change (as yellowing), occurrence of cracks or presence of efflorescences. Generally, this is more likely to happen when oil paintings are not optimally preserved but exposed to incorrect environmental conditions, like temperature variation or high relative humidity, or even under ultraviolet light [25].

All these phenomena may cause an evident alteration of pictorial layer and therefore they represent an issue for the conservation state of the work of art. Moreover, these phenomena appear more frequent in modern formulations that being commercial products, as mentioned before, they contain various additives that were not present in traditional paints and therefore they react in new ways with the organic structure of the oil [11].

An example can be the formation of metal salts (or metal soaps). They are commonly lead and zinc soaps, but also copper- and potassium-based; bound to saturated fatty acid like stearic, palmitic or azelaic acids, or also unsaturated fatty acids like oleic acid [26]. They are produced by the reaction between part of the free fatty acids present in aged oil paint and the metal ions of some pigments or driers (such as zinc or lead white) present in the paint or added to improve its properties [22], [27], [28]. These metal soaps are deposited on the surface, and they undergo to remineralization whose products are determined by the atmospheric conditions to which the painting is exposed. They can appear as organic efflorescences or crystalline and thick crusts

making sometimes the painting partially unreadable [29]. Moreover, some metal ions in pigments can be activated by ultraviolet light producing carbon dioxide and monoxide, dicarboxylic acids or VOCs causing the breakage of the paint layer and chalking.

Oil paint films particularly degraded present also an increase of sensitivity to solvent due to the higher proportion of lower molecular weight components, and chromatic variations as yellowing phenomena [8]. This latter is a characteristic phenomenon that occurs in drying oils already during their curing. It depends particularly on the presence of chromophores and the abundance of unsaturation, e.g., the presence of more linolenic acid than oleic and linoleic acid, as in linseed oil. The latter is in fact the oil that dries faster and at the same time turns yellow more. This color change can cause an alteration of the appearance of the painting, and it give rise to conservation issues.

1.1.5. The action of drying pigments on the polymerization process

As extensively discussed in previous paragraphs, the mechanism of drying of oils is very complex, and it is influenced by many factors. Among these, the thickness of the oil film, the presence of particular metallic ions or the presence of driers and antioxidants are fundamental [18], [30]. The thickness of the film affects the drying process because the thicker the layer, the longer it will take for the oil to cure completely and not just superficially. In fact, the superficial layers create like a barrier which prevents the oxygen uptake [8]. It takes 80-100 years to complete polymerization. Thus, to increase the rate of oxidation and improve the polymerization even of the innermost layers, already in ancient times, certain pigments were added intentionally to oil formulation as driers, similar to what is done today with oil colour tubes [25]. It was already know that some pigments containing transition metals are capable to influence the speed of drying process due to their catalyst action [18], [31]. The best oxidation catalysts include cobalt, chromium, manganese, copper, iron, and lead in this order. However, traditionally, the most commonly used driers were lead-based pigments like lead white (basic lead carbonate) [14].

Driers can accelerate the drying behavior of an oil in different ways, that is increasing oxygen uptake through catalysis, or reducing the induction period through precipitation or deactivation of antioxidants present in the oil [32], [33]. Depending on which phase of the oil drying process these metal salts act as driers, the metal ions have been divided in different categories:

- **Primary driers** (mainly Co^{2+}, Mn^{2+}, Ce^{3+}, V^{3+}, and Fe^{2+}) act during oxidation by catalysing the decomposition of hydroperoxides produced by the reaction between oil and oxygen, promoting the formation of free radicals and the subsequent bonds between

polymer chains [34], [35]. They must be multivalent, with more than one oxidation state [32].

- **Secondary driers** (mainly Pb^{2+}, Zr^{4+} and Al^{3+}) are mainly metal salts having only one oxidation state, as auxiliary driers. They are active during the polymerization phase, and they are responsible for the overall drying of the entire paint layer because they act deeper into the oil layer. They are usually used together with primary driers also to increase the rate of oxygen uptake [34].
- **Auxiliary driers** (Ca^{2+}, K^{+}, Li^{+}, and Zn^{2+}) mainly modify the activity of primary driers, improving their stability.

During the initiation step metal ions can react directly with the substrate changing their oxidation state from a higher state (M^{n+1}) to a lower state ($M^{(n+1)+}$) due to the electron transfer and thus starting the radical-chain reaction, according to the following reaction:

$$RH + M^{n+1} \rightarrow R^{\bullet} + M^{(n+1)+} + H^{-} \quad (5)$$

Then they promote the decomposition of hydroperoxides via a reduction-oxidation reaction called Haber and Weiss mechanism (6) (7), which can favour polymerization even in anaerobic conditions [35], [36].

$$ROOH + M^{n+} \rightarrow RO^{\bullet} + M^{(n+1)+} + OH^{-} \quad (6)$$

$$ROOH + M^{(n+1)+} \rightarrow ROO^{\bullet} + M^{n+} + H^{+} \quad (7)$$

$$2ROOH \xrightarrow{M^{n+}/M^{(n+1)+}} RO^{\bullet} + ROO^{\bullet} + H_2O \quad (8)$$

The ability of metal salts to catalyze oil oxidation and form films depends on both the solubility and dissociation of metal ions in the oil [32], [37]. Indeed, to have a sufficient concentration of metal ions to actually catalyze oil oxidation, the metal ions must be added separately or the they must be dissolved from the pigment itself [38].

When added intentionally as driers to the oil formulation, these metal salts have to be introduced to a maximum of 0.1%/w to maintain a good quality of paint. For example, in today's commercial formulations, lead-based driers are added in the range from 0.5%/w to 1.0%/w and it is often combined with other metal driers, but the concentration of the lead-based drier is usually much higher than that of other added driers [32]. In fact, it is known that it is fundamental to use a mix of driers to obtain uniform drying. Indeed, it is necessary the addition of a secondary/auxiliary drier, like Zn^{2+}, along with a primary drier, such as Co^{2+}, because the latter acts more on the surface, at the interface between the pictorial layer and the atmosphere,

leaving the substrate soft. Instead, secondary/auxiliary driers act deeper in the oil film contributing to polymerize the bulk of the oil paint, with a process called trough-drying [32].
It is possible to affirm that today the most commonly used driers are cobalt- and zinc-based compounds. Indeed, among the transition metals, cobalt appears to be the most effective and it almost replaced lead as main drier, with manganese, when lead toxicity was established in the mid-20th century [32], [39].
Thanks to different studies, it is possible to classify these metal ions according to their catalytic action [32], [36], as follows:

$$Co > Cr > Mn > Cu > Fe > V > Ni > Ti > Pb = Ca = Ag = Zn > Al > Mg = Cd$$

Observing the rank, it is possible to notice that lead is one of the least effective driers even if there are many variables to consider when determining dryer performances, like the diversity of tested compounds and the system used as study model [40]. Over the years, lead-based compounds have been relegated to the role of auxiliary driers, but lead can be actually considered both primary and auxiliary drier because it acts both on oxidation and polymerization process, on the surface but also in the bulk of the oil paint [22], [32]. Moreover, it is known that lead allows primary driers like cobalt-based compounds to maintain their efficiency during oxidation time; indeed, it seems that cobalt-based driers become inactive after a relatively short oil oxidation time, probably due to the formation of carboxylic acids.
Additionally, in modern and contemporary formulations, titanium dioxide and zinc oxide can be found, separately or in combination, because they have replaced white lead as pigments [35]. They also can act as drying pigments given to the catalyst properties of both metal ions.

1.2. The company Jacques Blockx

The Blockx brand was founded in 1865 in Belgium, and precisely in Nandrin (about 20 km from Liège), by Jacques Blockx I. He was a chemist and passionate about colours and pigments who started to produce traditional colours for some of his Belgian artist friends when due to the industrial revolution and other developments, artists no longer produced colours in their ateliers. The Blockx company counts painters like Paul Signac, René Magritte, Fernand Khnopff, Camille Pissarro, James Ensor, and Salvador Dalí as its most famous customers even though it has never been demonstrated by scientific analyses.

Today, this brand is recognized worldwide for the quality of its oil colours and the uniqueness of certain products, such as *Ambre dessous* by Blockx, which is a painting medium to mix to oil paint, really famous and appreciated among artists.

This product is mentioned and described in the book entitled "Compendium. À l'usage des artistes peintres et des amateurs de tableaux" which was published by Jacques Blockx I himself in 1892 in Paris [41]. It is a manual where he addressed various fundamental topics about painting, such as the choice of pigments, their compatibility with each other and the binder, or the use of varnishes, the choice of supports and the causes of oil alteration. Even today, this book is considered the true legacy of Jacque Blockx I and his knowledge of the chemistry of art.

1.1.6. Salvador Dalí and Blockx pictorial materials

Salvador Dalí (1904-1989) was a Spanish painter who belonged to the figurative side of the surrealist movement. He defined his own painting as "critical-paranoid"; an expression that can be translate as "looking at one object and seeing, thus painting, another" [42].

Surrealism was a multidisciplinary and organised movement born in 1924 thanks to André Breton (1896-1966). The aim of Surrealist art was to bring out a type of knowledge that could express the complexity of the human psyche. From a technical point of view, this was expressed in two strands: by experimenting innovative techniques, or by painting with traditional means dreamlike subjects, that were inspired by imaginary scenes and that, in any case, always contained elements that were incongruous with respect to the representation of reality [42].

His painting "The temptation of Saint Anthony" (dated 1946 - Royal Museum of Fine Arts of Belgium in Brussels), which will be presented in this thesis as case study, accurately represent this artistic technique.

Dalí's painting technique is very peculiar. His paintings are complex and detailed. His attention to detail was meticulous, almost maniacal. His painting is sharp and extremely finished, inspired by rigour and mastery, typical of the geniuses of the past like Vermeer, the Van Eyck brothers, Leonardo, and Raphael. Therefore, precisely in order to redeem painting from the vacuity of modern art, Salvador Dali published a book in New York in 1948 entitled "50 Secrets of Magic Craftsmanship", in which the artist sets out to reveal some useful secrets for becoming a good painter, from the use of brushes to the careful selection of colours [1].
In this manual, he mentions for the first time the use of the «yellow liquid amber according to the formula arrived at by Blockx», describing it as «sublime» and the only worthy heir to linseed oil for overpainting. As the old Flemish painters, he states to use the liquid amber mixed with oil paint (one drop of amber to five of oil) for the glaze technique, the pure liquid amber as varnish, or just for the correction of errors or regrets while painting.
He also mentions the formula of « Dalí wasps-medium » which consists of a lipid binder made of equal parts of poppy oil, walnut oil, and rectified turpentine, slowly mixed with liquid yellow amber dissolved in aspic oil, in at a 5:1 ratio [1].

1.3. Characteristic components of Blockx oil tubes

As mentioned above, oil painting products by Blockx are know all over the world for their quality but mainly for the uniqueness of some of them.
Regarding oil color tubes, the company states that they are made with finely selected pigments from around the world which are slowly grinded on stone cylinders giving them unparalleled quality and purity. According to what reported by Blockx company and the compendium by Jacques Blockx, the lipid binder present in the formulation of their oil paint tubes is chosen to best suit the chemical composition and physical properties of each pigment, to achieve homogeneous drying and maximum solidity [41]. Therefore, if earth pigments are ground with linseed oil, other pigments like whites (mainly titanium and zinc white) and blues (e.g., cobalt, or cerulean blue) are mixed with poppyseed oil, which Jacques Blockx considered the best non-yellowing oil. As already known, this choice is due to the different properties of the drying oils. Indeed, linseed oil has great qualities but, under normal paint conservation conditions, away from direct sunlight, it turns yellow. This characteristic is not a problem for browns, because yellowing is almost imperceptible, but mixed with whites and blues it can completely change the way a painting is read over time. Moreover, in addition to the yellowing, also the smoothness of the paste is considered, because it is essential to work. It changes depending

also on the lipid binder. Indeed, colors ground with linseed oil are very structured, but they mix much more easily and take longer to work if they are ground with poppyseed oil.
The most famous product sold by Blockx is the *Ambre dissous* or "yellow liquid amber" mentioned by Salvador Dalí which is sold pure or as an amber based solution for painting, composed of pure amber, aspic essence, poppy oil, and turpentine, according to the description given by the company.
A paragraph of the compendium by Jacques Blockx entitled "De l'ambre dessous et de son application à la peinture artistique" is dedicated to this particular product. Blockx states that the dissolved amber (or succin) forms with the oil, which serves as a vehicle, a real combination. It is described essentially as a fat and elastic product, pure, shiny, and of the same color as the natural succin. He writes also that dissolved amber does not decompose. Indeed, after its solidification it does not change colour, and its desiccation is slow and regular. Blockx states that once it mixed with colors, there is no need to protect the finished work because the amber embedded in the painting act as a protective. It also gives a reflective effect to the colors, making them look more beautiful and transparent, brighter, and more intense at the same time. The dissolved amber is considered the secret of the Flemish masters of the 15th and 16th centuries, which was forgotten for centuries, and then it was rediscovered by Jacques Blockx around 1860. Indeed, in his compendium, Jacques Blockx reports a part of a manuscript by Théodore Turquet de Mayerne of 1620 in which the author cited the main painting methods used by painters of his time, namely Rubens and Van Dyck, and referring to a conversation he had with the latter, he wrote: « voice of a man who melted amber without breaking it, so that the dissolution was white, yellow, and transparent ». Blockx then reflects on the fact that reporting this note on dissolved amber testifies that de Mayerne must not have known how to dissolve this resin 'without burning it' and, moreover, must have attached great importance to this secret [41]. This note demonstrates that dissolved amber was in use even three hundred years ago and Blockx found a method to reproduce something whose good effect are proven by the amazing conservation of the Flemish school works of art.

1.1.7. Amber as binder in paintings

According to Jacques Blockx compendium, even if the use of amber as varnish has been known since antiquity, the use of amber as binder for painting has been attested from 15th century by Flemish painters. They used oil painting almost exclusively with local technical characteristics in the preparation of colors. The pigments were ground with a lipid binder, then hard resin (<70%/w) and sometimes also essential oil were added giving a particular consistency to the

colors [43]. In this way they were able to paint in successive layers, now dense and opaque, now transparent, and luminous, also in relation to the colored layer of the background. Therefore, resins were added to the painting medium to make colors appear more transparent and brighter, but mainly to slow the drying rate and improving viscosity of oils for glazing, in particular for the last layers of the painting [7]. At that time, before the introduction of synthetic resins, natural resins were used for this purpose, like ambers. However, it is essential to consider that the ancient term amber was probably attributed to many natural resins, including sandarac, mastic or colophony; therefore it must be considered that the excellent properties referred to amber could actually be due to other natural resins with which the paints were made [14]. For example, a recipe for the preparation of the Flemish medium reported by Jacques Maroger mentions the use of mastic varnish (60%wt of resin mastic and 40%wt of turpentine) mixed in 1:1 ratio with heated oil with 10%wt of litharge [44].

This is the reason why a description of the main characteristics of natural resins is necessary. In general, natural resins consist of a complex mixture of organic substances such as alcohols, carboxylic acids, ketones, polycyclic hydrocarbon structures (e.g., abietic or neoabietic acid), and aromatic components. The components are mainly of terpenoid origin [45].

Terpenes are hydrocarbon molecules, often polycyclic unsaturated, i.e., containing as their characterizing functional group the C=C double bond, which can be hydrated to form alcohols, and subsequently ethers. Whereas the methyl groups can be oxidized to aldehydes, carboxylic acids, and, in some cases, to ketones. Their molecular structure is multiple of a fundamental unity with five atoms of carbon, called “isoprene unit”, which in its simplest functional form it is isoprene (2-methyl-1,3-butadiene) (Error! Reference source not found.). These units are usually chained together in a head-to-tail arrangement, in linear or cyclic form [46].

Terpenoid compounds are basically infinite due to the presence of the double bonds and their configuration (E and Z), and the presence of other functional groups, mentioned above. Therefore, they have been divided into different groups depending on the number of constituent isoprene units. However, the most common terpenes of interest for art, conservation and restoration are mono- (C10), sesqui- (C15), di- (C20), and tri- (C30) terpenes (called terpenoids, if functionalized).

Natural resins commonly used in the artistic field comprise di- and triterpenoids which are not found together in the same resin, a useful characteristic for the purposes of chemical analysis [18]. Diterpenes are solids due to their high molecular weight and they are the main constituents of vegetable resins, among which the most common is colophony. These resins are composed of diterpenes consisting of a carboxylic group, called resin acids. The latter contain diterpenes

with three possible structures: abietic, pimaric and labdanic compounds (Error! Reference source not found.). Abietic and pimaric compounds are mainly present in *Pinacee* resins, like colophony; whereas labdanic compounds are constituents of *Cipressacee* resins, such as sandarac [46].

Triterpenes are characterized by a low degree of unsaturations compared to diterpenes. Their formation occurs cyclization of squalene oxide ((S)-squalene-2,3-epoxide) which first leads to the tetracyclic lanosterol, and euphol [46].

Mastic and Dammar are two common triterpenoid resins which have been often used as varnishes. Dammar derives from the family of trees *Dipterocarpaceae* and mastic derives from the genus *Pistacia* (*Anacardiaceae* family). Mastic is composed of a polymeric fraction (cis-1,4-poli-β-myrcene) and a non-polymeric one consisting of a large number of triterpenes. They are compounds with the skeleton of the eufan and the tetracyclic dammaran, and the pentacyclic oleanan and lupan; all compounds that form the soluble fraction of Dammar. The characteristic components of mastic are masticodienol acids and derivatives [46].

Regarding the amber, it is a fossil resin originated from the secretion of tall stem plants belonging to conifers (*Pinites succinifer*), now extinct, characterized by the ability to produce in large quantities and that have been fossilized for millions of years [18]. The most well-known amber is Baltic amber (mineralogically known as succinite). It is mainly found in the "Blue Earth" formations on the Baltic coast of former East Prussia, with some now occurring in Poland. However, most of it is produced in Lithuania [18].

From the chemical point of view, Baltic amber contains the dicarboxylic acid succinic acid (1,4-butanedioic acid), both in its free and esterified state (1:1 ratio), which gives it the characteristic name succinite [18]. The proportion of free dicarboxylic acid groups gives the polymer some properties of an ion-exchange resin; instead, the esterification of succinic acid leads to crosslinking and therefore to the increase of average molecular weight and the subsequent increase of melting point and decrease of solubility.

It has the typical behavior of a high molecular weight cross-linked polymer, and in particular, it can be considered as a natural alkyd resin, the product of esterification of a polyvalent alcohol (co-polymer of communol and communic acid) with dicarboxylic acid (succinic acid).

Moreover, the soluble part of the amber contains monoterpenoids and diterpenoids, which can be in part analytically identified. The monoterpenoid fraction includes borneol, camphor, fenchyl alcohol and fenchone, and also compounds like fenchyl and bornyl hemisuccinates. Regarding the diterpenoid fraction, in addition to succin acid, amber contains small amounts of acid esters present in fresh conifer resins, such as 48-iso-pimaric acid (about 0,4%/w), whose

presence after millions of years is remarkable. The chemistry of the resin that makes up amber is actually more similar to *Araucaceae* family than to *Pinaceae* one; in fact, amber does not contain abietic acid [18].

1.1.8. Spike oil in oil painting formulations

As mentioned in the previous paragraph, spirits (also called essential oils) were added in painting medium to decrease the viscosity without modifying the rheological behaviour of the oil binder [43]. In particular, turpentine was used to this purpose, but according to Helme and Rodde, it may be spike oil [47]. It is also mentioned by Théodore de Mayerne in his manuscript in recipes for spirit varnishes, such as the one that instructs to dissolve sandarac resin in spike oil; or by the 16th century Italian artist Gian Paolo Lomazzo who recommended grinding pigments with « walnut oil, spike oil and other things » [48]. Also today, it is a commercial product for artists of brands like Franc Le bourgeois and Sennelier indicated for glazing, for the preliminary sketches and slowing the drying rate of oil.

In literature, spike oil is also called “essence of aspic” or “spike lavender” [49], [50]. It is distilled from the so called *Lavandula Spica*, a broad-leafed variety of lavender which grows wild in Europe and it is extensively cultivated in Spain [51]. This variety was first mentioned in the 12th century by Hildegard of Bingen in her book “Causae et Curae” [52]. Thank to Dorothy Chaytor in 1937, spike lavender was renamed *L. Latifolia*, and it has been distinguished by *L. Angustifolia* (true lavender). Nevertheless, in the writing of classical authors it is almost impossible to distinguish them.

The spike oil is the product of steam distillation of the flowers of spike lavender. It was considered inferior to lavender oil for perfumery and it was relegated to other uses [52].

From the chemical point of view, spike oil is an essential oil mainly composed of monoterpenoids compounds. The most abundant monoterpenes are 1,8-cineole, linalool, and camphor. In addition, also linalyl acetate (acetic ester of linalool) is present [53]. Its chemical composition is very different compared to that f *L. Angustifolia*, mainly for the higher camphor content in *L. Latifolia* [54].

The chemical properties of spike oil are similar to turpentine since they are both products of distillation. They are excellent solvents for vegetable oils and natural resins; however, spike oil evaporates slower than turpentine and it has been recommended for use in addition to the varnishes. It is known that if turpentine accelerates the drying process of oil painting, essential oils such as spike oil slow down it [55], [56].

2. Materials and methods

2.1. The Blockx mock-ups under study (set1 and set2)

Two uniform sets of samples made with selected Blockx commercial oil paints have been prepared for the first phase of the research consisting of characterization and monitoring over time of the Belgian company pictorial products. The Blockx products available for this study are eight tubes of oil paints and three amber-based painting solutions (**Table 3**). Among the oil paints, three of them (*Blanc de Titane*, *Blanc de Zinc* and *Vert Émeraude*) are recent, from 2010, and the other five are considered "historical": the precise date of production is not known, but they are still from the 20th century. Regarding the amber-based painting solutions, they are currently manufactured and sold by Blockx. As reported on the label, the *Solution d'ambre à l'huile de lin* consists of dissolved normal amber (*ambre dessous normal*) and linseed oil in a ratio of 1:10. As stated on the Blockx catalogue, the *Solution à peindre 25 ml* consists of pure amber, poppy oil, aspic oil and turpentine; and the *Solution à peindre 10 ml* has the same composition as the *Solution à peindre 25 ml* with a surplus of turpentine (70% solution à peindre and 30% turpentine).

The mock-ups have been prepared by applying a little amount of pictorial product on a Melinex® polyester film (4 or 5 cm x 10 cm) and by spreading it with a thickness of 100 µm by means of a BYK bar applicator, according to the procedure developed under project MIMO (Metal Ion Migration mechanisms in oil paints drying and degradation) [57].

A first set (set1) consisting of 11 samples was obtained by applying all the oil paints and the three amber-based painting solutions on the Melinex® film (see **Table 3**).

A second set (set2) of 3 samples was obtained by mixing an oil paint with the *Solution à peindre 25 ml* with a 5:1 ratio In particular, *Blanc de Titane, Bleu de Cobalt* and *Vert de Cobalt* have been chosen as oil paints (see **Table 4**). This second set was prepared following the references in the literature both for the components and the proportion. As mentioned earlier, in his book Salvador Dalí reported the recipe for his « wasps-medium » prepared with poppy oil, walnut oil and rectified turpentine mixed with yellow amber dissolved in aspic oil [1]. For this reason, *Solution à peindre 25 ml* was chosen to prepare the second set of mock-ups, given the presence in it of most of these ingredients and thus the similarity to what Dalí called « wasps-medium ». Regarding the proportion, the Spanish painter recommended mixing the oils with amber in aspic oil in a 5:1 ratio. Moreover, in one of the Blockx brochure of the *Ambre dissous* (dissolved amber) the company suggests the use of amber together with the oil in proportion of one drop

of amber per five of oil. Instead, regarding the three oil paints used for the mix with the amber-based solution 25 ml, they were chosen based on the colors most present in the painting "The temptation of Saint Anthony" by Salvador Dalí, from the results of previous non-invasive in situ analysis [2].

Table 3 The set1 Blockx mock-ups (11 samples) made by applying the eight oil paints and the three amber-based painting solutions on a Melinex® film.

Table 4 The set2 Blockx mock-ups (3 samples) obtained by mixing three oil paints with *Solution à peindre 25 ml* with a 5:1 ratio.

2.2. Experimental methods

The Blockx oil paint mock-ups (set1 and set2) have aged under natural light and ambient temperature inside the laboratory for seven and five months, respectively.

In order to gather information on the composition and film-forming processes over time of the mock-ups, a multi-analytical approach was adopted. In particular, attenuated total reflection infrared spectroscopy (ATR-FTIR), gas chromatography-mass spectrometry (GC-MS) and percentage weight variation calculation have been performed.

For the characterization of the oil paints, XRF, micro-Raman and FTIR-ATR have been used mainly to identify the nature of the organic binder used in Blockx products and the presence of inorganic components such as pigments or additives. GC-MS was useful to characterize the binding media and identify the presence of other organic components present in the formulations. For the monitoring over time during the drying process of oil paint mock-ups, both ATR and GC-MS have been used to observe the chemical changes of the lipid binder, i.e., the organic products formed during the auto-oxidation, hydrolysis, and curing. Furthermore, percentage weight variation has been carried out to implement this study monitoring the drying behaviour, in particular the duration of drying phases.

As shown in **Table 5**, set1 was monitored for a seven-month aging time, while set2 for a period of five months. ATR and GC-MS have been performed together from 0h to the last measuring, except for 24h and 72h when only ATR has been carried out, due to the analytical timing.

Regarding the monitoring of percentage weight variation, it was carried out for both sets three times a day for the first three days, then once a week for the first month and finally every month until the end of the monitoring period (**Table 6**).

Table 5 ATR (x) and GC-MS (x) analysis performed on set1 and set2.

	0h	24h	48h	72h	1w	2w	3w	4w	2m	3m	4m	5m	6m	7m
set1	x x	x	x x	x	x x	x x	x x	x x	x x	x x	x x	x x	x x	x x
set2	x x	x	x x	x	x x	x x	x x	x x	x x	x x	x x	x x		

Table 6 Monitoring of percentage weight variation carried out on set1 and set2.

	0h	3h	6h	24h	27h	30h	48h	51h	54h	72h	75h	78h	1w	2w	3w	4w	2m	3m	4m	5m	6m	7m
set1	x	x	x	x	x	x	x	x	x	x	x	x	x	x	x	x	x	x	x	x	x	x
set2	x	x	x	x	x	x	x	x	x	x	x	x	x	x	x	x	x	x	x	x		

2.3. Analytical techniques

2.3.1. Optical Microscopy (OM)

Optical microscopy analysis was performed for observing the seven samples taken from the 20th century painting " The temptation of Saint Anthony " by Salvador Dalí (see **Table 36**). A bench microscope ZEISS SteREO Discovery.V8 (Carl Zeiss Microscopy GmbH) was used, which is a modular microscope equipped with a manual 8:1 zoom, a manual or motorized focus and two ZEISS Achromat S Objectives of 0.63× and 1.5×. For this research, the 1.5× objective was used. The digital camera used by the microscope is a ZEISS Axiocam 208 color full 4K resolution at 30 fps. Images were collected by using the ZEISS ZEN core 3.6 software.

2.3.2. Energy Dispersive X-Ray Fluorescence (EDXRF)

XRF spectra were acquired by means of a compact, portable, and high-performance micro-XRF scanning spectrometer Bruker CRONO which allowed non-contact punctual analysis of samples. The target material is rhodium anode, a 1mm collimator, and the spot diameter was about 0.5-1 mm depending on the analysis point. The measurement was carried out by fixing voltage at 27kV and a current of 150μA with a duration of 180s, exploring a field of analysis from 1 to 27 keV. To properly interpret the obtained data, the X-ray transition application (RaySpec X-ray Spectroscopy) was used.

2.3.3. Scanning Electron Microscopy with Energy Dispersive X-ray spectroscopy (SEM-EDX)

For this research, SEM-EDX analysis were performed on two cross-sections by means of JOEL JSM 5600LV scanning electron microscope coupled with the EDX detector Oxford

Instruments ISIS Series 300 with a resolution of 133 eV @ MnKα (5.9 keV). The microscope has an Everhart-Thornley's detector for secondary electrons (SE), tension of acceleration between 1 to 30 kV.

Before the analysis, the two selected samples were embedded in light-curing resin (Technovit® 2000 LC). After curing under UV-lamp, the resin-embedded samples were polished on one side with increasing fineness (200–4000 grains/cm2) on a polishing machine using water as a lubricant and then with polishing pads (8000 and 12,000 grains/cm^2).

2.3.4. Micro-Raman spectroscopy

Raman spectra were retrieved using a Thermo ScientificTM DXR3TM dispersive Raman system (Waltham, MA, USA) equipped with an Olympus microscope. The experimental parameters were laser wavelengths of 785 nm, laser power in a range of 0.4-20 mW depending on the sample analyzed and full range grating 50-3325 cm^{-1}. A 10x, 50x and 100x objective and a slit aperture of 25 μm were used to obtain more representative spectra from the samples. The total acquisition time for each spectrum was 120 s. Thermo ScientificTM OMNICTM 34.3 software (version 3, Waltham, MA, USA) was used to operate the DXR3TM Raman microscope and to collect the spectra. Raman spectra were compared both with the instrument's internal library and the literature for peak assignment.

2.3.5. Attenuated Total Reflection Infrared Spectroscopy (ATR-FTIR)

For the research, a Bruker Optics Alpha spectrophotometer in ATR mode was also used, with a diamond crystal capable of investigating a sample area of 0.75 mm at a depth of around 1 μm. The spectrometer was equipped with a Pt/SiC globar source, a RockSolid interferometer (with gold mirrors), and a deuterated triglycine sulfate (DLaTGS) detector, operating at room temperature and giving a linear response in the spectral range between 7500 and 375 cm^{-1}. The background was measured before each analysis and spectra were recorded between 4000 and 400 cm^{-1} by performing 48 scans, with a resolution of 4 cm^{-1}. Data acquisition was managed through OPUS software (Version 8.2.28). The spectra were further elaborated using OriginPro 8.5 and Thermo Nicolet's OMNIC 6.0. Since the support of the mock-ups is composed of a material undetectable by IR radiation (Melinex®), no sampling was necessary from the second monitoring week. The mock-ups were simply placed in direct contact with the crystal.

2.3.6. Gas Chromatography Mass Spectrometry (GC-MS)

The GC-MS analysis was performed by using Thermo Scientific™ TRACE™ 1300 Series GC System equipped with an ISQ 7000 MS with a quadrupole analyzer (ThermoFisher Scientific, Waltham, MI, USA). Samples were injected by a AS1310 autosampler in splitless mode at 280°C and GC separation was performed on a chemically attached fused silica capillary DB–5MS Column (30 m length, 0.25 mm, 0.25 µm—5% phenyl methyl polysiloxane), using helium as the carrier gas (1 mL/min flow rate). The MS interface and the inlet temperature were both set to 280°C. The transfer line was at 280°C and the MS source temperature was 300°C. The temperature was programmed from 80°C to 315°C with a ramp of 10°C, held isothermally for 2 minutes; the total runtime was 27.50 minutes. The temperature interference was at 280°C, while MS was run in Full Scan mode (m/z 50-600) with a speed of 0.2 scan/sec. The volume injected was 1 µL and the solvent delay was set at 8 minutes. The MS was conducted at 1.9 scans per second in full scan mode (*m*/*z* 40–650). Electron Ionisation energy was 70 eV. Data were acquired and processed by means of Chromeleon chromatography studio 7.

According to a procedure developed by Izzo [8], the microsamples (approximately 0.3 mg) have been sampled with a scalpel, weighted and placed into micro vials, then, after the addition of 10µl of internal standard (C19), they have been transesterified using 30 µl of 3-(Trifluoromethyl)phenyltrimethylammonium hydroxide (5% in methanol); after the reaction taking place overnight in accordance with the methodology presented in [3, 4], 150 µl of methanol have been added.

The qualitative interpretation was performed by analyzing the mass spectrum of each compound by comparison with NIST library. Using nonadecanoic acid as the internal standard (10 µL of 1 mM nonadecanoic acid in a methanol solution in each of the micro vials), quantitative analysis could also be performed.

2.3.6.1. GC-MS quantitative analysis

Due to the inconstant sensitivity of the instrument, it is necessary to correct the concentrations obtained by means of response factors (RF) of fatty acids, glycerol, and internal standard. Therefore, prior to the analysis standard solutions have been prepared. Three different solutions have been prepared considering the composition of linseed oil: glycerol (GLY), saturated fatty acids (SFA), and unsaturated fatty acids (UFA). Methanol was used as solvent for all the three solutions, and MethPrepII™ as derivatizing agent. These three solutions have been prepared by adding 10 µl of external standard (GLY, SFA and UFA respectively), 10 µl of internal

standard (C19, nonadecanoic acid) and 30 µl of MethPrepII™. After 24 hours at room temperature, 120 µl of methanol have been added.

The RF is determined starting from standard solutions of known concentration subjected to GC-MS analysis under the same conditions as the samples, according to the formula:

$$RF = (As^* Cis) / (Ais^* Cs) \quad (9)$$

in which

RF= Response Factor
As= Area of the target
Ais= Area of the internal standard
Cs= Concentration of the target
Cis= Concentration of the internal standard

Regarding the response factor of glycerol, it was calculated by the sum of the area of each derivative present in the solution following then the equation (1).

After the calculation of the RF, the concentration of fatty acid methyl esters was calculated by using the following equation:

$$C_x = (A_x^* C_{is}) / (A_{is}^* RF) \quad (10)$$

in which

Cx= Concentration of the compound (mmol/mL)
Ax= Area of the analyzed compound
Cis= Concentration of the internal standard
Ais= Area of the internal standard
RF= Response Factor

Since, this value of concentration is related to the methyl ester form of the correspondent fatty acid, the conversion factor from methyl ester to fatty acid is considered. Thus, the fatty acids concentrations were calculated as follows:

$$[FA] = (A_{ME}^* W_{Mis}^* MW_{FA}) / (A_{Mis}^* W_S^* MW_{ME}) \quad (11)$$

in which

[FA]= concentration of fatty acid
A_{ME}= Area of the fatty acid ME (methyl ester)
A_{Mis}= Area of internal standard
W_{Mis}= weight of the internal standard added
W_S= weight of the sample (mg)
$MW_{FA=}$ molecular weight of the fatty acid
MW_{ME}= molecular weight of corresponding methyl ester

As final step the percentage of each fatty acid related to the sum of all the fatty acids contained in the sample was calculated using the following formula:

$$\%[FA] = ([FA] / \Sigma[FA]) * 100 \quad (12)$$

Then the following fatty acid molar ratios were determined and used as parameters to characterize the kind of lipidic binding media and to observe the degree of oxidation [8], [60]–[63]:

- **P/S** (palmitic-to-stearic acid ratio) that is conventionally used for the identification of traditional drying/non-drying oils [18]; P/S= 1.7 for linseed oil, P/S > 3 for poppy seed oil and P/S= 2.6 for walnut oil. This evaluation was based on the statement that saturated fatty acid, such as palmitic and stearic, do not undergo modifications during the curing of an oil. Recent studies, however, have proven that the possible decrease of P/S with ageing is due to the preferential loss of palmitic acid with respect to stearic;
- **A/P** (azelaic acid-to-palmitic acid ratio) is a parameter that is normally used to distinguish drying oils from egg lipids; A/P > 1 for oils and A/P < 0.3 for egg.
  In fact, as already said in (par. 1.1.3), high amounts of dicarboxylic acids, and azelaic in particular, are registered in aged drying oil as they are formed during the auto-oxidation of the unsaturated fatty acid (linolenic, linoleic, and oleic acids) present in drying oils. A/P ratio is strongly influenced by several factors, such as the rate of oxidation, degradation and polymerisation; the age of the paint; the pre-heating treatments during oil preparation; the presence of pigments and driers.
- **D/P** (the total sum of dicarboxylic acids-to-palmitic acid ratio) also provides an assessment of the degree in drying processes, as difatty acids are more abundant in aged films.
- **ΣD** (the total sum of dicarboxylic acids) that is also used to determine the type of lipid binder;
- **O/S** (oleic acid-to-stearic acid ratio) is the ratio between an unsaturated fatty acid (C18:1) and a saturated fatty acid (C18:0) and it is useful to define the maturity of an oil film. This value is an index of oxidation since the unsaturated acid is particularly reactive to oxygen when oil film is exposed to air. It is known from literature that O/S ratio for aged films is around 0.1-0.2, as oleic content is rather low.
- **A/Sub** (azelaic acid-to-suberic acid ratio) (or **2C9/2C8**) can provide an assessment of any preheating processes that may have occurred in the preparation of the oil. If A/Sub > 6, the oil is considered crude, i.e., not preheated, whereas a value between 2 and 3 could refer to a preheated oil, i.e., pre-polymerization of the binding material.

2.3.6.2. Pyrolysis-GC-MS qualitative analysis

Considering that this study is also aimed at identifying some possible markers of Blockx products and comparing them with samples taken from Salvador Dalí's painting, the pyrolysis GC-MS approach was also used. In fact, as mentioned above, the three paint solutions from the Blockx company under study are expected to contain terpene-based compounds, including mono-, di- and triterpenoids; and it is known that GC-MS gives poor results because only the low molecular weight fraction, which is mainly composed of labdane type molecules and sandaracopimaric acid, can be identified.
To determine the nature and composition of the cross-linked fraction analytical pyrolysis is required.

2.3.7. Percentage weight variation

In addition to ATR-FTIR and GC-MS analyses, the calculation of percentage weight variation was performed on set1 and set2 Blockx mock-ups to study the drying behaviour and monitor the chemical and physical processes which occur during the drying time. In fact, thanks to this tool it is possible to observe the duration of induction period, the maximum weight gain respect to the original weight, and the loss of volatiles after gelling [23]. This calculation has been performed according to the formula:

$$\Delta\text{Weight }\% = [(X_f - X_i) / X_i] \times 100\% \quad (13)$$

in which

X_i = initial value of the weight
X_f = final value of the weight

This percentage calculation is always performed between the previous weight and the next weight and so on in a chain. For this research, a technical balance was used to weight the oil paint films and, then the values of ΔWeight % were used to create line graphs with time and average percentage value on the x-axis and y-axis, respectively. For each oil paint mock-up, three weighings have been made for the accuracy of the result, so as to obtain three drying curves to compare.

3. Results and discussion

3.1. Characterization and study of film behaviour over time

In this chapter the results of the study of the Blockx oil paint mock-ups (set1 and set2) prepared in laboratory is presented. The study has been carried out by means of XRF, micro-Raman, ATR-FTIR, GC-MS, and the calculation of the percentage weight variation over time.
Since most of the Blockx mock-ups mainly consist of a lipid binder mixed with an inorganic pigment, a reference table of the main absorptions related to the different fractions observed by means of ATR-FTIR and one with the main organic compounds found via GC-MS have been reported in **Appendix A** (**Table A*1*** and **Table A2**).

3.1.1. Blockx oil paint mock-ups set1

3.1.1.1. Blanc d'Argent Moyen

Blanc d'Argent Moyen by Blockx is described by the company as lead carbonate (PW1) mixed with linseed oil. Indeed, by observing the ATR-FTIR spectrum of the fresh oil paint (Error! Reference source not found.) it is possible to observe the main peaks related to the presence of a lipid binder at 2955, 2917, and 2848 cm^{-1} attributed to the stretching vibrations of CH_3 and CH_2 groups of fatty acids. In addition, the absorption of the stretching mode of C=O at 1733 cm^{-1}, the small peak at 3012 cm^{-1} and the one at 721 cm^{-1} referred to the stretching and bending modes of the C=C-H unsaturated bonds are also visible [64], [65]. Other minor peaks are at 1652, 1171 related to C-O stretching vibration and 1105 cm^{-1} to the O-CH_2-C asymmetric stretching [66].
XRF measurement showed the dominant presence of lead suggesting the use of basic lead carbonate ($(PbCO_3)_2 \cdot Pb(OH)_2$) as corroborated by the ATR-FTIR spectrum. The latter exhibits a strong absorption at about 1350 cm^{-1} and the sharp peak at 1043 cm^{-1} attributed to the asymmetric and symmetric stretching of CO_3^{2-}. It is also possible to observe the characteristic peak at 3533 cm^{-1} related to the stretching vibration of OH group [67]. Then, also other bending modes of carbonate group in the region between 900 and 400 cm^{-1} at 851, 835, 765 cm^{-1}, with a maximum at 676, 397 and 358 cm^{-1} are present.
Regarding the film formation process, in Error! Reference source not found. the graphical representation of the percentage weight variation over time of the *Blanc d'Argent Moyen* mock-up is reported. During the first 6 hours after layering, it is possible to observe a positive weight change due to the initial uptake of atmospheric oxygen by the carbon-carbon double bonds

which usually starts in the first hours of the drying process after an induction period [21]. Already after 24 hours, the oil paint film loses weight (about 1.60%) as a result of the evaporation of volatile molecule formed by oxidation and molecular rearrangements [23]. Then the drying curve seems to stabilize until the end of monitoring period.

By observing the ATR-FTIR spectra acquired during the monitoring period, it is possible to notice that in the first 24 hours, some critical changes occurred (Error! Reference source not found.). In particular, the intensity of the peak at 3012 cm^{-1} and the small one at 721 cm^{-1} (mostly covered by the absorptions of the inorganic pigment) attributed to unsaturated bond C=C-H and typical of a young oil film is reduced considerably suggesting that during the first day most of the unsaturated fatty acids reacted with oxygen producing active radical species to start the autoxidation process [7]. The peak at 3012 cm^{-1} totally disappears within 2 months.

It is also possible to observe that the broad band at about 3400 cm^{-1} (not registered at 0h) increases over time, mainly due to the alcohol and/or hydroperoxide groups formation during the polymerization and ageing processes [8], [68].

In addition, during the ageing process also the small peak at 2955 cm^{-1} decreases becoming a small shoulder at the end of monitoring period and the characteristic peak at 1733 cm^{-1} related to the ester stretching C=O becomes broader due to the hydrolysis of triglycerides and the formation of other oxidation/degradation products like aldehydes, ketone, anhydrides and free fatty acids [8].

These changes at the early 24 hours confirm that the drying process has proceeded very fast likely enhanced by the presence of lead in the composition of the pigment. It is in fact known that lead has siccative properties and it can be considered both primary and secondary drier due to its action both on the surface and in the bulk of the oil paint film [22], [32].

The GC-MS analysis allowed to study more deeply the composition of the lipidic binder and the change of the molecular composition by detecting and monitoring the presence of unsaturated and saturated fatty acids and the oxidation products formed during the drying and curing process. In **Figure 2**, it is possible to observe the comparison of two chromatograms, the first at 0 hours and the last one at 7 months.

As the ATR-FT-IR spectra which are characterized by the typical absorption peaks of lipidic binder, the GC-MS analyses show the presence of the characteristic compounds of drying oils (as methyl esters, because the solutions have been derived during sample preparation [7], [8]): glycerol derivatives, unsaturated (as oleic C18:1, linoleic C18:2 and linolenic C18:3) and

monosaturated fatty acids (such as myristic C14, palmitic C16, stearic C18), and dicarboxylic (such as azelaic 2C9, suberic 2C8, sebacic 2C10) fatty acids were detected.

Figure 2 GC-MS chromatograms of *Blanc d'Argent Moyen* after 0 hours (left) and after 7 months (right)

Table 7 Retention time (min), molecular ion (m/z) and name of each compound detected at 0h and 7 months in Blanc d'Argent Moyen by Blockx mock-up.

Retention time (min)	Molecular ion M^+ (m/z)	Fatty acid ME 0 hours	Fatty acid ME 7 months
9.65		-	Pentanoic acid, 4-oxo
10.00		-	Octanoic acid, 8-hydroxy
10.19	89	Glycerol 89	Glycerol 89
10.40	162	Glycerol 162	Glycerol 162
10.48	172	Nonanoic acid, 9-oxo	Nonanoic acid, 9-oxo
10.61	202	Suberic acid	Suberic acid
10.75		Phthalic acid	Phthalic acid
10.88	75	Glycerol 75	Glycerol 75
11.26		-	Methyl 10-oxo-8-decenoate
11.39		-	Terephtalic acid
11.54	200	-	Decanoic acid 9-oxo
11.87	216	Azelaic acid	Azelaic acid
13.05		-	Sebacic acid
13.90	241	Myristic acid	Myristic acid
14.38		-	Aleuritic acid
15.40	394	Glycerol 394	Glycerol 394
15.77		-	Octanedioic acid, 3,5-dimethyl
15.96		Palmitoleic acid	-
16.00	270	Palmitic acid	Palmitic acid
16.77		-	3-oxo-1,8-octanedicarboxylic acid
17.63		Palmitic acid, 14-methyl	-
17.63	292	Linoleic acid	Linoleic acid
17.69	296	Oleic acid	Oleic acid
17.91	298	Stearic acid	Stearic acid
18.19	294	Linolenic acid	Linolenic acid
18.81	312	Nonadecanoic acid	Nonadecanoic acid
19.49		-	Stearic acid, 9-oxo
19.55		Eicosanoic acid	-
19.67		-	Stearic acid, 12-hydroxy
19.80	134	Glycerol main	Glycerol main
21.29	354	-	Behenic acid

Table 7 lists the compounds detected at 0h and 7 months with their retention time and molecular ion. After seven months, different compounds can be observed such as oxidation

products in different form like oxo- and hydroxy-, and dicarboxylic acids which are the main oxidative degradation products formed as results of fragmentation of triglycerides. The oxidation products formed during the propagation reactions are already present after 1 week the preparation of the mock-up.

The concentration of the main fatty acids present over time in the *Blanc d'Argent Moyen* mock-up are reported in **Table 8**, allowing to do some general considerations about the molecular changes occurring during the drying process. In particular, it is possible to affirm that unsaturated fatty acids such as oleic, linoleic, and linolenic acid decrease already within the first 48 hours and this continues until the end of the monitoring period, when almost the absence or a low concentration of UFAs can be detected. Moreover, an increase of the concentration of the dicarboxylic acid azelaic, and the appearance of suberic and sebacic acid already at the first GC-MS monitoring at 48 hours can be observed. It is possible to notice that a low concentration of dicarboxylic acids like azelaic and suberic acid has been found also at 0h, suggesting that the oil paint *Blanc d'Argent Moyen* has undergone a slight oxidation due to the catalytic effect of lead present in the formulation and the fact that the oil tube was not closed well. This can be confirmed by the sticky consistency during the application of the film.

Regarding the molar ratios reported in **Table 9**, other considerations can be made about the drying process and the polymeric film formation [63]. Regarding A/P ratio, it is possible to observe that the concentration of azelaic acid is a bit low compared to the other oil paint that will be presented in the next paragraphs, and the A/P ratio after 7 months is 0.75. This can be attributed to the difficulty in spreading the color because of the pasty consistency of the oil color in question, and that therefore did not allow the drafting of a perfect 100 µm film as for the other colors. Indeed, the thickness of the painting film affects the polymerization of the lipid film.

Oil binder can be characterized as linseed oil mixed with other oils like safflower or sunflower since the P/S ratio after 7 months is 2.43. In fact, pure linseed oil is identified with P/S=1.5-1.8, walnut with P/S=2-2.6 and poppy seed with P/S >3 [18]; nevertheless, modern paint manufacturers commonly employ several kinds of drying, semi-drying and non-drying oils whose P/S values are often overlapped [8], [69].

Furthermore, after 7 months A/Sub ratio is >6 (precisely 9.05) suggesting that the oil used was not pre-heated.

It is possible to observe that A/P and D/P ratios increase over time due to the increase of dicarboxylic acids in the oil composition. O/S is an index of the maturity of the film; indeed, an aged film shows a O/S around 0.1-0.2. After 7 months this ratio is still high (2.02) suggesting

that the that film is not completely dried. Finally, %D continues to increase until seven months showing that the polymerization of the film is taking place.

Table 8 Concentration (µg/mg) of the main fatty acids present over time in the Blanc d'Argent Moyen.

FA	Concentration over time (µg/mg)								
	0h	48h	1w	2w	4w	2m	4m	6m	7m
Oleic acid	15.41	13.60	10.76	10.39	9.27	8.36	6.50	6.52	6.03
Linoleic acid	19.19	4.31	2.77	2.48	1.68	1.10	0.97	0.88	0.60
Linolenic acid	2.04	1.05	0.79	0.70	0.65	0.63	0.63	0.54	0.54
Suberic acid	0.05	0.07	0.28	0.09	0.15	0.44	0.40	0.37	0.61
Azelaic acid	0.75	1.84	1.93	2.05	2.50	4.24	4.01	4.22	5.49
Sebacic acid	0.00	0.00	0.05	0.13	0.15	0.21	0.23	0.02	0.41

Table 9 Molar ratios of some fatty acids and %D changing over time in the Blanc d'Argent Moyen.

Molar ratios	Molar ratios and D% over time								
	0h	48h	1w	2w	4w	2m	4m	6m	7m
A/P	0.10	0.14	0.22	0.29	0.29	0.53	0.66	0.66	0.75
D/P	0.11	0.14	0.27	0.32	0.32	0.61	0.76	0.72	0.90
O/S	4.05	1.76	2.41	2.71	1.85	2.02	2.29	2.11	2.02
%D	1.55	4.53	7.22	7.74	9.31	16.78	19.87	19.72	24.49

3.1.1.2. Blanc de Titane

By observing the spectrum in Error! Reference source not found. and according to the ATR-FTIR absorptions reported in **Table A1**, the *Blanc de Titane* by Blockx consists of a lipid binder mixed with an inorganic pigment which has been characterized by means of micro-Raman spectroscopy. It is a titanium white (PW6) consisting of titanium dioxide (TiO_2) in rutile form since its main absorptions occur at 139, 227, 440 and 603 cm^{-1} (Error! Reference source not found.) [70].

Regarding the drying processes of the oil paint film, the percentage weight variation of the mock-up is reported in Error! Reference source not found.. The drying curve appears instable until the first month of monitoring period showing a weight gain in the first hours after the preparation of the film and as for the *Blanc d'Argent Moyen* a weight loss within 24 hours due to the initial uptake of oxygen and then the first removal of volatile compounds mentioned before. During the second day, it is possible to notice another weight gain of about 1,50% and then an increase in stability from the third day is observed.

The ATR-FTIR spectra acquired during the 7 month ageing (Error! Reference source not found.) show important changes in the molecular composition of the oil film from the first 24 hour monitoring analysis and a certain stability after 72 hours. It is possible to notice a decrease of the peak at 3011 cm^{-1} which suggests the decrease of unsaturation within the oil composition, and the broadening of the carbonyl peak at 1744 cm^{-1} due to the hydrolysis of triglycerides and the formation of low molecular weight degradation products like aldehydes and ketones [8]. The intensity of the broad band 3378 cm^{-1} increases already after 24 hours and continues more and more until the first month when also the intensity of all the spectral shape decrease [71].
In addition, it is possible to observe an increase of the peaks at 1239 and 1098 cm^{-1} characteristic of the ester bonds (C-O) after 48 hours . The carbonyl peak also seems to decrease in intensity from 72 hours as the characteristic peaks at 2923 and 2854 cm^{-1} which undergo a noticeable decrease in intensity from the third day of ageing.
From 4 weeks to 7 months any other changes can be noticed in the ATR-FTIR spectra (Error! Reference source not found.) as it can be observed also in the drying curve of the percentage weight variation reported in Error! Reference source not found. where any important weight changes can be detected.

The variation of the molecular composition over time has been observed and studied also by means of GC-MS. In Error! Reference source not found., the two chromatograms at 0 hours and 7 months are reported. Comparing them, it is possible to notice the significant increase of dicarboxylic acids, but also the formation of new products, such as oxidation products in oxo- and hydroxy- forms.

The results of the quantitative analysis are reported in **Table 10** and **Table 11**. In the first one, the concentration of the main fatty acids present over time is presented, allowing to do some general considerations about the molecular changes occurring during the drying process. In particular, it is possible to observe that changes due to oxidative polymerization occurs within the first week, when there is a strong decrease of unsaturated fatty acids i.e., oleic, linoleic, and linolenic acid and an increase of dicarboxylic acids. As before a little amount of azelaic acid was already present in the oil composition at 0 hours, due to the fact that the oil paint tube was not sealed but was already open.
Regarding the molar ratios reported in **Table 11**, other considerations can be made about the drying process and the polymerization state but also about the nature of the oil binder. The

value of A/P ratio is <1 in the first period due to the low amount of azelaic acid in the oil, however this value stabilizes within two months. The lipidic binder could be characterized as mixture of linseed oil and other drying/semi-drying oils, such as like safflower or sunflower since the P/S ratio at 7 months is 2. The presence of safflower could be confirmed by the high amount of eicosanoic acid in the fresh oil paint (Error! Reference source not found.) [8]. Furthermore, A/Sub ratio<6 over time suggests that the oil binder was thermally treated. Regarding the drying process, D/P ratio and %D continue to increase until seven months after a strong increase within the first week showing that the polymerization of the film is still taking place.

Table 10 Concentration (µg/mg) of the main fatty acids present over time in the Blanc de Titane.

FA	Concentration over time (µg/mg)								
	0h	48h	1w	2w	4w	2m	4m	6m	7m
Oleic acid	30.78	21.15	7.77	5.67	4.43	2.60	1.46	0.34	0.50
Linoleic acid	37.03	23.09	0.18	0.11	0.22	0.19	0.03	1.42	0.20
Linolenic acid	3.84	1.95	2.01	1.31	1.08	0.79	0.84	0.72	0.74
Suberic acid	0.00	0.00	1.31	0.71	1.31	2.67	2.00	2.41	3.20
Azelaic acid	0.78	0.84	8.59	9.13	8.72	11.73	9.45	9.78	13.78
Sebacic acid	0.00	0.00	0.39	0.32	0.41	0.74	0.54	0.65	0.90

Table 11 Molar ratios of some fatty acids and %D changing over time in the Blanc de Titane.

Molar ratios	Molar ratios and %D over time								
	0h	48h	1w	2w	4w	2m	4m	6m	7m
A/P	0.06	0.07	0.82	0.64	0.86	1.12	1.12	1,16	1.18
D/P	0.06	0.07	0.99	0.75	1.03	1.45	1.42	1.53	1.54
O/S	4.78	3.84	1.42	1.17	0.71	0.50	0.36	0.08	0.09
%D	0.80	1.12	23.45	20.58	27.63	36.92	38.64	40.32	40.53

3.1.1.3. Blanc de Zinc

ATR-FTIR spectrum of *Blanc de Zinc* by Blockx (Error! Reference source not found.) exhibits the main peaks of a drying oil, as reported in **Table A1**. XRF measurement detected only Zn, therefore it is possible to affirm that the white pigment is zinc white (PW4) consisting of zinc oxide (ZnO) which has been also characterized by means of micro-Raman spectroscopy. The spectrum shows a strong peak at 432 cm^{-1} and another at 331 cm^{-1} (Error! Reference source not found.) [70].

Regarding the film drying process, in Error! Reference source not found. the drying curve of Blanc de Zinc mock-up is reported. It shows some instability consisting in weight gain and

weight loss until the first week, when the weight does not change anymore until the seventh month.

In the first six hours the curve appears almost flat suggesting a period of induction due to the natural antioxidants present in the oil composition, i.e., the tocopherols [21]. After 24 hours it is possible to notice a weight loss and then after 48 hours a considerable weight gain of about 2.00%. This unusual drying curve can be explained by the reduced weight of the *Blanc de Zinc* film mock-up compared to other oil paints and the difficulty for the operator of establishing the correct weight at each weighing due to fluctuations on the analytical balance.

By observing the FTIR-ATR spectra acquired from 0 hours until 7 months, in fact, it is possible to notice a normal drying process which starts already after 24 hours and continues at least until the first week where important changes can be detected (Error! Reference source not found.). The band at 3417 cm^{-1} appears more visible after 24 hours due to the formation of hydroperoxides and alcohols in the first phase of oil curing. The peak at 3006 cm^{-1} and the one at 720 cm^{-1} decrease as the reaction of UFAs with the atmospheric oxygen occurs, almost disappearing after 72 hours [17], [23]. At the same time the characteristic peak at 1747 cm^{-1} begins to widen after 24 hours suggesting that the hydrolysis of triglycerides is occurring [8]. In addition, between 24 and 48 hours the intensity of the peaks at 1653 and 1555 cm^{-1} increases becoming a single broad band; and just after 48 hours the peak at 2955 cm^{-1} begins to decrease.

In Error! Reference source not found., the two chromatograms acquired at 0 hours and 7 months are reported. After seven months, several compounds can be found in addition to unsaturated fatty acids and glycerol derivatives, such as fatty acids with a lower molecular weight, oxidation products in different form like oxo- and hydroxy-, and dicarboxylic acids. In particular, oxidation products appear already within the first week.

As for the *Blanc de Titane* mock-up, the molecular composition of oil film changes consistently within the first week (**Table 12**). In fact, it is possible to observe a strong decrease of unsaturated fatty acids and the increase of dicarboxylic acids, especially of azelaic acid, which it is known to be the most produced one because it is the result of the oxidative cleavage of the double bond at the C9 position of the three unsaturated fatty acids with eighteen atoms of carbon (oleic, linoleic, and linolenic acids) [23].

By observing the molar ratios in **Table 13**, it is possible to notice a general increase over time of A/P, D/P and %D, except O/S due to the increase of dicarboxylic acids in the oil

composition. After seven months these values show a certain stability showing that the polymeric network of the film is formed even if the complex drying process lasts years.
Regarding the nature of oil binder, it is possible to affirm that the paint tube contains a drying oil since A/P ratio stabilizes around 1 after two months. Moreover, it can be characterized as mixture of linseed oil and other drying/semi-drying oils since P/S after 7 months is 2.29, similar to *Blanc de Titane*. Furthermore, A/Sub ratio is <6 after 7 months suggests the use of a pre-heated oil.

Table 12 Concentration (µg/mg) of the main fatty acids present over time in the Blanc de Zinc mock-up.

FA	Concentration over time (µg/mg)								
	0h	48h	1w	2w	4w	2m	4m	6m	7m
Oleic acid	22.59	20.14	8.74	5.17	2.69	1.59	1.00	1.14	1.47
Linoleic acid	32.36	26.05	0.11	0.14	0.36	0.15	0.03	0.12	0.08
Linolenic acid	1.89	1.24	1.95	1.41	0.59	0.68	0.80	0.69	0.71
Suberic acid	0.00	0.00	1.13	0.64	1.23	2.58	2.21	2.30	3.39
Azelaic acid	0.46	0.91	8.23	5.81	9.21	11.21	9.62	9.59	13.78
Sebacic acid	0.00	0.00	0.35	0.22	0.40	0.65	0.53	0.61	0.86

Table 13 Molar ratios of some fatty acids and %D changing over time in the Blanc de Zinc mock-up.

Molar ratios	Molar ratios and %D over time								
	0h	48h	1w	2w	4w	2m	4m	6m	7m
A/P	0.04	0.07	0.72	0.63	0.85	1.12	1.11	1.19	1.16
D/P	0.04	0.07	0.85	0.72	1.00	1.44	1.43	1.56	1.51
O/S	3.81	3.87	1.59	1.20	0.51	0.35	0.26	0.28	0.28
%D	0.55	1.22	21.35	20.25	29.38	38.40	38.78	41.36	38.46

3.1.1.4. Bleu Coeruleum

The oil paint *Bleu Coeruleum* by Blockx consists of PB35 (cobalt stannate, Co_2SnO_4) mixed with a drying oil. The ATR-FTIR spectrum exhibits the main absorption peaks related to a lipid binder, according to the **Table A1** (Error! Reference source not found.Error! Reference source not found.). Regarding the inorganic pigment, cobalt and tin have been detected by means of XRF; furthermore, both Raman and ATR-FTIR spectroscopy have allowed to clearly identify the compound. ATR-FTIR spectrum shows two peaks at 639 and 512 cm^{-1}. Raman spectrum exhibits the two typical peaks of cerulean blue at 525 and 666 cm^{-1} (Error! Reference source not found.) [70].

The drying curve of this oil paint mock-up shows the typical weight gain in the first hours due to the oxygen uptake by the UFAs present in the fresh oil followed by a weight loss after 24 hours because of the decomposition and loss of volatile compounds as a result of oxidation reactions (Error! Reference source not found.) [24]. Then, during the second day until the third one, little fluctuations of the weight can be noticed, however some stability of the film mass can be observed already after about four days until the end of monitoring period.

This fast drying process can be observed also by the FTIR-ATR spectra acquired during the monitoring period shown in Error! Reference source not found.. In fact, all the characteristic changes in the infrared spectral shape occur within 24 hours and then any other changes can be observed. The peak at 3006 cm^{-1} and the one at 2955 cm^{-1} disappear showing the decrease of unsaturated fatty acids in the oil composition. The carbonyl peak at 1744 cm^{-1} becomes broader than before suggesting that the hydrolysis of triglycerides is occurred during the first day since the peak does not undergo to any other changes. In addition, also the intensity of the broad band at 3362 cm^{-1} increases within 24 hours and continues to widen until the first month due to the presence of alcohol and hydroperoxide groups formed as a result of film formation during the polymerization and ageing processes [8].
It is known that certain pigments which contain some particular metal ions can promote the oxidation and/or polymerization process of the oil film [35], [36], [40], [72]. In this case, the presence of cobalt, which is the most effective catalyst among transition metals, has certainly speeded up the drying process by promoting the radical-chain reaction and the successive decomposition of hydroperoxides via redox reactions favouring the polymerization [35], [36].

In Error! Reference source not found., the two chromatograms acquired at 0 hours and 7 months are reported. After seven months, different compounds can be found. In particular, oxidation products appear already within the first week. In this case, the consistent decrease of unsaturated fatty acids occurs within the first 48 hours, as it is possible to observe in **Table 14** and **Table 15**. To confirm that the drying process is occurring, there is also an increase of dicarboxylic acids, especially of azelaic acid. By observing the molar ratios in **Table 15**, it is possible to notice a general increase over time of A/P, D/P and %D. After seven months these values show a certain stability showing that the polymeric network of the film is formed even

if the complex curing process, especially in the bulk of the paint, is a phenomenon that continues for many years, until all the polyunsaturated bonds in TAGs disappear [17], [22]. As already mentioned above, the fast drying process occurring already within the first 24 hours can be associated to the presence of cobalt ion in the formulation.

Regarding the nature of oil binder, it is possible to affirm that the paint tube contains a drying oil since A/P ratio stabilizes around 1 after two months. Moreover, it can be characterized as mixture of linseed oil and other drying/semi-drying oil since P/S after 7 months is 2.83, similar to the oil paints investigated previously. Furthermore, A/Sub ratio is ~3 after 7 months suggesting the use of a boiled oil.

Table 14 Concentration (µg/mg) of the main fatty acids present over time in the Bleu Coeruleum mock-up.

FA	Concentration over time (µg/mg)								
	0h	48h	1w	2w	4w	2m	4m	6m	7m
Oleic acid	18.79	7.19	2.36	2.05	1.29	0.98	0.55	0.59	0.96
Linoleic acid	29.19	0.11	0.12	0.13	0.35	0.11	0.07	0.11	0.19
Linolenic acid	1.65	0.39	0.81	0.66	0.27	0.43	0.31	0.24	0.30
Suberic acid	0.00	0.54	2.05	1.18	1.72	3.14	3.26	3.28	4.81
Azelaic acid	0.69	5.53	9.45	7.44	9.90	10.08	11.06	10.71	14.93
Sebacic acid	0.00	0.00	0.52	0.41	0.36	0.56	0.62	0.62	0.90

Table 15 Molar ratios of some fatty acids and %D changing over time in the Bleu Coeruleum mock-up.

Molar ratios	Molar ratios and %D over time								
	0h	48h	1w	2w	4w	2m	4m	6m	7m
A/P	0.06	0.47	0.96	0.78	0.96	1.06	1.23	1.27	1.29
D/P	0.06	0.52	1.22	0.95	1.16	1.45	1.67	1.74	1.79
O/S	3.50	1.82	0.58	0.49	0.27	0.21	0.15	0.17	0.23
%D	0.95	17.35	32.81	28.99	35.67	39.33	44.59	47.24	47.08

3.1.1.5. Bleu de Cobalt

Bleu de Cobalt by Blockx is composed of a lipid binder, as it is possible to observe in the ATR-FTIR spectrum reported in Error! Reference source not found., and the blue pigment cobalt blue (PB28) which is cobalt aluminate ($CoAl_2O_4$). The pigment has been identified thanks to the presence of typical strong peaks at 487, 541 and 640 cm^{-1} [73]. Moreover, it is possible to observe an absorption at 1574 cm^{-1} which can be attributed to a metal carboxylate, probably

calcium stearate, added as stabilizer to prevent the separation of the oil medium from the pigment(s) [26], [74].

By observing the graphical representation of the percentage weight variation (Error! Reference source not found.), it is possible to notice that the drying process of *Bleu de Cobalt* was very fast, similarly to *Bleu Coeruleum* paint probably due to the presence of the cobalt ion (Co^{2+}) in the oil paint formulation. The drying curve shows an increase in mass during the first six hours and then the loss of mass due to the evaporation of volatile compounds within the first day. Then only some weight fluctuations occur and then it stabilize already after the first three days as the *Bleu Coeruleum*. Nevertheless, it is possible to observe that the weight gain is of about 4%. The percentage weight variation is an indication of the amount of UFAs that react with atmospheric oxygen [23]. This high percentage could be explained by the fact that the oil/pigment ratio in the color formulation is likely higher than other oil paints under study. This hypothesis is due to the fact that the consistency of this oil color during application on the Melinex® film was much oilier than the others.

The catalytic effect of the cobalt ion is also visible in the spectral shapes of FTIR-ATR spectra reported in Error! Reference source not found.. The characteristic changes that suggest that the drying process is in progress occur in the first two days. The peak at 3013 cm^{-1} and the one at 2958 cm^{-1} decrease until they disappear within 48 hours. At the same time, the formation of the broad band at about 3400 cm^{-1} attributed to the O-H groups occurs within 24 hours and increases over time until the end of the monitoring period. In addition, already after 24 hours the carbonyl peak at 1743 cm^{-1} is wider than before and also the peak at 1574 cm^{-1} associated to the presence of metal soaps increases becoming a broad band until the seventh month.

The GC-MS analysis allowed to study the oil composition during the drying process. In Error! Reference source not found., the two chromatograms acquired at 0 hours and 7 months are reported. After seven months, it is possible to observe several compounds in addition to those present at 0 hours suggesting that the drying process took place. In particular, oxidation products appear already within the first 48 hours. In fact, within 48 hours some changes in the

amount of UFAs and dicarboxylic acid can be observed (**Table 16**). After 1 week the concentration of dicarboxylic acids increases more and sebacic acid appears. The oil film behavior of *Bleu de Cobalt* appears similar to that of *Bleu Coeruleum* probably due the influence of cobalt ion present in the oil formulation.

Regarding the molar ratios in **Table 17**, it is possible to notice a general increase over time of A/P, D/P and %D. After seven months the variation of these values appears very low suggesting that the two main phases of the drying process occurred. As already mentioned above, the fast drying process occurring already within the first 24 hours can be associated to the presence of cobalt ion in the paint formulation.

Regarding the nature of oil binder, A/Sub ratio is 4.17 after 7 months suggesting the use of pre-heated oil. P/S ratio is 1.08 after 7 months suggesting the presence of metal stearates which lower the ratio in question [11].

Table 16 Concentration (µg/mg) of the main fatty acids present over time in the Bleu de Cobalt mock-up.

FA	Concentration over time (µg/mg)								
	0h	48h	1w	2w	4w	2m	4m	6m	7m
Oleic acid	31.49	25.83	12.07	12.03	8.52	6.60	4.40	4.70	5.12
Linoleic acid	6.63	3.82	0.26	0.26	0.27	0.23	0.05	0.12	0.08
Linolenic acid	7.46	0.44	2.35	2.45	1.08	1.13	1.25	1.55	1.55
Suberic acid	0.00	0.15	1.94	1.12	1.32	2.57	2.87	3.13	4.09
Azelaic acid	0.42	6.67	11.61	8.67	11.47	13.20	12.76	13.08	17.04
Sebacic acid	0.00	0.00	0.97	0.77	0.61	1.22	1.19	1.34	1.75

Table 17 Molar ratios of some fatty acids and %D changing over time in the Bleu de Cobalt mock-up.

Molar ratios	Molar ratios over time (%)								
	0h	48h	1w	2w	4w	2m	4m	6m	7m
A/P	0.03	0.47	0.95	0.73	0.99	1.22	1.29	1.31	1.34
D/P	0.03	0.48	1.19	0.95	1.16	1.57	1.70	1.76	1.79
O/S	2.61	2.03	1.18	1.05	0.80	0.65	0.47	0.49	0.43
%D	0.50	9.31	23.30	18.25	25.39	30.76	33.66	34.76	35.13

3.1.1.6. Vert de Cobalt

Vert de Cobalt by Blockx consists of a drying oil mixed with the inorganic pigment cobalt green (PG50) (Error! Reference source not found.). XRF measurements detected cobalt and zinc confirming the presence of cobalt green which is composed of cobalt(II) zincate

(CoO·nZnO). In addition, micro-Raman spectrum exhibited three peaks at 432, 460 and 596 cm^{-1} attributed to cobalt and zinc oxides [75].

The graphical representation of the percentage change variation shows the typical weight gain in the first hours after the layering and then a weight loss within 24 hours (Error! Reference source not found.). During the second day of ageing, it is possible to observe some fluctuations of the weight which are not present from the third day onwards. As seen before for *Bleu Coeruleum* and *Bleu de Cobalt*, it is possible to hypothesize that the drying process occurred very fast probably due to the presence of the primary drier Co^{2+}. In this case Zn^{2+} is also present, which acts as auxiliary drier improving the efficiency and the stability of the primary one, by acting deeper in the oil layer contributing to polymerize the bulk of the oil paint [32].

The infrared spectra acquired during the monitoring period confirm that the drying process occurred so fast (Error! Reference source not found.). In fact, already in the first day, the characteristic peak related to presence of unsaturated fatty acids 3008 cm^{-1} decreases. The carbonyl peak at 1745 cm^{-1} becomes wider and its intensity decreases in the first 24 hours. Also, the peaks at 1647 and 1569 cm^{-1} increase to form a single broad band over time since 24/48 hours. In addition, the peak at 2954 cm^{-1} almost disappears within two days. From 1 month to the end of monitoring, any other changes can be observed.

Also by means of GC-MS analysis, it is possible to notice this fast drying process. In Error! Reference source not found., the two chromatograms at 0 hours and 7 months are reported. Comparing them, it is possible to notice the significant increase of dicarboxylic acids at the expense of unsaturated fatty acids, but as seen before also the formation of new products like oxidation products in different forms.

The results of the quantitative analysis are reported in **Table 18** and **Table 19**. It is possible to observe that a radical change in the oil composition occurs within the 48 hours when the second GC-MS analysis has been performed. There is a strong decrease of the amount of unsaturated fatty acids especially linoleic acid which goes from 28.32 to 1.06 µg/mg, followed by an increase of dicarboxylic acids. Suberic acid appears within 48 hours, while sebacic acid is detected in the first week after the preparation of the mock-up. The little amount of azelaic acid already present in the oil at 0 hours can be due to the fact that the oil paint tube was already opened, as seen before for example for *Blanc d'Argent Moyen* and *Blanc de Titane*.

Considering the molar ratios reported in **Table 19**, it can be confirmed the presence of a drying oil due to the value of A/P ratio >1, which can be characterized as a mixture of linseed oil and other drying oils since P/S ratio after 7 months is 2.76. Furthermore, A/Sub ratio=5.03 suggests that the oil binder can be pre-heated.

Table 18 Concentration (µg/mg) of the main fatty acids present over time in the Vert de Cobalt mock-up.

FA	Concentration over time (µg/mg)								
	0h	48h	1w	2w	4w	2m	4m	6m	7m
Oleic acid	17.12	11.16	4.71	3.90	2.67	1.66	1.38	1.16	1.75
Linoleic acid	28.32	1.06	1.05	0.12	0.41	0.10	0.07	0.13	0.09
Linolenic acid	2.52	0.94	0.97	0.97	0.71	0.49	0.59	0.49	0.74
Suberic acid	0.00	0.33	0.92	0.66	0.88	1.73	1.52	1.53	2.02
Azelaic acid	0.30	5.03	6.97	5.61	7.05	8.70	7.74	7.72	10.16
Sebacic acid	0.00	0.00	0.26	0.29	0.24	0.38	0.36	0.39	0.51

Table 19 Molar ratios of some fatty acids and %D changing over time in the Vert de Cobalt mock-up.

Molar ratios	Molar ratios and %D over time								
	0h	48h	1w	2w	4w	2m	4m	6m	7m
A/P	0.03	0.49	0.78	0.65	0.79	1.02	1.02	1.07	1.02
D/P	0.03	0.53	0.91	0.76	0.92	1.27	1.26	1.34	1.28
O/S	3.25	2.44	1.29	1.06	0.57	0.49	0.46	0.37	0.49
%D	0.44	13.85	25.71	23.89	28.76	37.75	27.98	41.30	38.60

3.1.1.7. Vert de Cobalt Foncé

Vert de Cobalt Foncé by Blockx is composed of drying oil and cobalt green (Error! Reference source not found.), according to the infrared absorptions reported in **Table A1**. The presence of the inorganic pigment was confirmed also by the XRF measurement which showed the presence of cobalt and zinc.

Regarding the drying behavior of this oil paint, the curve of the percentage weight variation is reported in Error! Reference source not found.. In the first six hours after the preparation of the mock-up, it shows an unusual weight loss of about 4%. Then an increase of the weight within 24 hours and a consequent weight loss of about 3%. After two days, the weight stabilizes until it no longer varies from the first week onward.

The infrared spectra acquired during the monitoring show a very fast drying process which appears very similar to the one of *Vert Cobalt* previous investigated (Error! Reference source

not found.). In fact, within the first 24 hours, the peak related to presence of unsaturated fatty acids 3007 cm^{-1} decreases. The carbonyl peak at 1744 cm^{-1} becomes wider and its intensity decreases in the first 24 hours.

The intensity of the peak at 2954 cm^{-1} decreases after 24 hours, almost disappearing within two days. Also, the peaks at 2920 and 2852 cm^{-1} decrease after 48 hours. A broad band at about 1600 cm^{-1} is formed after the first day, due to the increase of intensity of 1651 and 1571 cm^{-1} peaks attributed to the COO- bending of fatty acids. From the third week the broad band at about 3400 cm^{-1} almost disappears and any other changes can be observed.

In Error! Reference source not found., the two chromatograms acquired at 0 hours and 7 months are reported. The last chromatogram appears more complex due to the formation of different products during the oxidation and polymerization process. In particular, oxidation products appear already within the first week. While the consistent decrease of unsaturated fatty acids followed by the increase of dicarboxylic acids occurs within the first 48 hours, as it is possible to observe in **Table 20**. Suberic acid appears within 48 hours and sebacic is visible in the 1 week chromatogram, suggesting that the oxidation is in progress. %D increases from 0.53 to 25.03% in the first 48 hours (**Table 21**). As already mentioned above, the fast drying process occurring already within the first 24 hours can be associated to the presence of cobalt ion in the formulation.

Regarding the nature of oil binder, the presence of a drying oil is confirmed by the A/P ratio which stabilizes around 1 after two months. Moreover, this lipid binder can be identified as mixture of different oils typical of modern oil paint formulations since P/S after 7 months is 2.71, similar to the oil paints investigated previously. Furthermore, A/Sub ratio after 7 months is 3.08 suggesting the use of a boiled oil.

Table 20 Concentration (µg/mg) of the main fatty acids present over time in the Vert de Cobalt Foncé mock-up.

FA	Concentration over time (µg/mg)								
	0h	48h	1w	2w	4w	2m	4m	6m	7m
Oleic acid	18.04	6.84	1.98	1.71	1.33	0.84	0.83	0.70	1.09
Linoleic acid	28.91	0.27	0.30	0.41	0.40	0.27	0.29	0.24	0.25
Linolenic acid	2.55	1.54	1.15	0.80	0.07	0.43	0.45	0.33	0.42
Suberic acid	0.00	1.48	2.70	1.83	2.41	3.54	3.29	3.01	4.50
Azelaic acid	0.39	9.09	11.48	8.76	11.39	11.62	10.65	9.77	13.85

Sebacic acid	0.00	0.00	0.67	0.55	0.53	0.64	0.62	0.66	0.91

Table 21 Molar ratios of some fatty acids and %D changing over time in the Vert de Cobalt Foncé mock-up.

Molar ratios	**Molar ratios and %D over time**								
	0h	**48h**	**1w**	**2w**	**4w**	**2m**	**4m**	**6m**	**7m**
A/P	0.03	0.80	1.07	0.84	1.03	1.19	1.21	1.23	1.17
D/P	0.03	0.92	1.39	1.06	1.29	1.61	1.66	1.69	1.62
O/S	3.31	1.30	0.41	1.37	0.29	0.22	0.23	0.19	0.25
%D	0.53	25.03	37.75	32.91	40.01	44.73	44.62	47.67	44.09

3.1.1.8. Vert Émeraude

Vert Émeraude by Blockx is composed of a mixture of drying oil and viridian (PG18) as it is possible to observe in the ATR-FTIR spectrum (Error! Reference source not found.). The infrared spectrum exhibits indeed its characteristic peaks at 1285, 1249, 1061, 791, 695, 678, 541, 466, 477, 422 cm^{-1} [76]. XRF measurement showed the presence of chromium confirming the use of viridian which consists of hydrated chromium oxide ($Cr_2O_3 \cdot H_2O$).

Regarding the drying processes of the oil paint film, the percentage weight variation of the mock-up is reported in Error! Reference source not found.. The drying curve appears slightly instable until the first three days of monitoring period showing a weight gain in the first hours after the preparation of the film and a weight loss within 24 hours due to the initial uptake of oxygen and followed by the first removal of volatile compounds mentioned before. During the second day, some fluctuations occur and then an increase in stability from the third day is observed.

The ATR-FTIR spectra acquired during the seven month ageing (Error! Reference source not found.Error! Reference source not found.) show important changes in the molecular composition of the oil film from the first 24 hour monitoring analysis and a certain stability after 72 hours like it has been observed in the drying curve. Already within 24 hours, it is possible to notice a decrease of the peak at 3006 cm^{-1} which suggests the decrease of unsaturations within the oil composition, and the broadening of the carbonyl peak at 1744 cm^{-1} due to the hydrolysis of triglycerides and the formation of low molecular weight degradation products like aldehydes and ketones [8]. After 48 hours the peak at 3006 cm^{-1} disappears completely. In addition, the strong peak at 1163 cm^{-1} related to the C-O stretching of esters increases the intensity and becomes broader.

From the first week to 7 months any other changes can be noticed in the ATR-FTIR spectra as it can be observed also in curve of the percentage weight variation reported in Error! Reference source not found. where any important weight changes can be detected.

In Error! Reference source not found., the two chromatograms acquired at 0 hours and after 7 months are reported. Dicarboxylic acids are present in high amount respect to unsaturated fatty acids and moreover oxidation products and low molecular weight compounds can be found.
By observing the concentration of the main fatty acids changing over time, it is possible to affirm that the consistent decrease of long-chain unsaturated fatty acids occurs within the first week (**Table 22**). At the same time dicarboxylic acids increase, especially azelaic which continues to increase even after 7 months showing that the drying process is still occurring. The low concentration of UFAs after 7 month suggests that the oxidation is still occurring but at lower rate. Suberic acid appears within 48 hours, while sebacic acid can be detected in the chromatogram acquired after 1 week. The molar ratios reported in
Table 23, show a general increase over time of A/P, D/P and %D, as mentioned before. Considering O/S ratio it is possible to affirm that after 7 months the film can be considered aged since normally O/S for aged oil is around 0.1-0.2.
Regarding the nature of oil binder, P/S ratio = 1.73 after 7 months suggesting the presence of linseed oil. Moreover, A/Sub ratio is 2.45 which can be attributed to a pre-heated oil.

Table 22 Concentration (µg/mg) of the main fatty acids present over time in the Vert Émeraude mock-up.

FA	Concentration over time (µg/mg)								
	0h	48h	1w	2w	4w	2m	4m	6m	7m
Oleic acid	27.09	26.19	11.65	8.53	3.89	1.73	1.28	1.22	1.75
Linoleic acid	52.25	12.49	0.44	0.30	0.55	0.17	0.17	0.05	0.33
Linolenic acid	4.14	0.60	1.91	1.01	1.36	0.53	0.46	0.57	0.47
Suberic acid	0.00	0.24	1.96	2.29	3.64	7.20	7.56	7.91	12.13
Azelaic acid	0.54	5.84	12.33	11.49	18.52	20.40	19.66	19.58	29.67
Sebacic acid	0.00	0.00	0.51	0.90	0.99	1.61	1.67	1.73	2.57

Table 23 Molar ratios of some fatty acids and %D changing over time in the Vert Émeraude mock-up.

Molar ratios	Molar ratios and %D over time								
	0h	48h	1w	2w	4w	2m	4m	6m	7m
A/P	0.03	0.34	0.70	0.78	1.10	1.27	1.42	1.43	1.45

D/P	0.03	0.36	0.95	1.00	1.38	1.82	2.09	2.14	2.17
O/S	2.56	3.09	1.30	1.05	0.39	0.20	0.15	0.14	0.15
%D	0.43	7.59	24.20	26.02	35.84	43.53	47.30	51.48	46.47

3.1.1.1. Solution d'ambre à l'huil de lin (Amber solution with linseed oil)

The *Solution d'ambre à l'huil de lin* by Blockx is mainly composed of drying oil as it is possible to observe in the ATR-FTIR spectrum reported in Error! Reference source not found.. The presence of a natural resin is difficult to detect only by means of infrared spectroscopy due to the similar main chemical groups of both materials, such as methyl, methylene, carbonyl, ester, and hydroxyl groups. Natural resins, among which there are also fossils resins like amber, show different characteristic features in the infrared region. There are three wavenumber domains of interest for amber, namely those between 2000-3600 cm^{-1}, 1350-1820 cm^{-1} and the 1045-1250 cm^{-1}regions [77]. In the case of Blockx paint solutions, it is possible to affirm that the spectral shape can be associated to the oil component, like the previous Blockx oil paints. The CH_2/CH_3 stretching vibrations normally occurring between 3000-2840 cm^{-1}, also for natural resins, in this binder solution are visible at 2922, 2852 and 2955 cm^{-1} (Error! Reference source not found.).

Resins normally show also a distinctive broad band in the 2700-2500 cm^{-1} range due to O-H stretching of a dimerized carboxyl group and a typical carbonyl of aldehydes and ketones stretching band near 1700 cm^{-1} and specifically between 1715 and 1695 cm^{-1} [78], [79].

These specific bands are visible in the infrared spectrum of paint solutions by Blockx. Specifically, for the *Solution d'ambre à l'huil de lin* it is the peak at 2675 cm^{-1} and the one at 1709 cm^{-1} (Error! Reference source not found.).

The graphical representation of the percentage weight variation during the drying process shows the typical weigh gain of about 2% in the first hours after the layering and then a weight loss after 24 hours (Error! Reference source not found.). Then the curve shows some weight fluctuations until the third day to become stable until the end of the monitoring period. This behavior can be seen also through the infrared spectra reported in Error! Reference source not found. acquired from 0 hours to 7 months, where some stability can be observed after one week. The main changes in the molecular composition of the oil film occur within 72 hours.

Indeed, the intensity of the broad band at 3455 cm^{-1} increases within the first day and this phenomenon continues until 1 week, due to the formation of alcohol and hydroperoxides groups. Moreover, the carbonyl peak at 1738 cm^{-1} becomes wider with the formation of degradation products such as aldehydes, ketones, and free fatty acids by the hydrolysis of triglycerides. In addition, the intensity of the peak at 1167 cm^{-1} related to the C-O stretching of esters increases. The contribution of the unsaturated fatty acids to the oxidation process can be seen with the decrease of the peak at 3008 cm^{-1} and the one at 724 cm^{-1} which are attributed to the unsaturated bond C=C-H. This decrease is visible between 48 and 72 hours after the preparation of the mock-up.

In Error! Reference source not found., two chromatograms acquired at 0 hours and 7 months are reported. They are very complex chromatograms for the presence of a terpene fraction which will be discussed in **par. 3.3**. Regarding the drying process, after seven months, different compounds can be found like oxidation products that appear already within the first week.
Considering the concentration of the main fatty acids, unsaturated and saturated, present in the oil over time, it is possible to notice that the consistent decrease of unsaturated fatty acids followed by the increase of dicarboxylic acids occurs within the first week (**Table 24**). The linoleic acid almost disappears after 7 months, while oleic acid is still present, suggesting that the drying process is still occurring. In fact, the O/S ratio, reported in **Table 25**, does not reach the 0.2-0.1 value as seen for most of oil paints previously investigated, but after 7 months it is 0.86. This may be due to the presence of the pure liquid amber in the paint solution as the company Blockx affirm. It is known in fact that natural resins slow the drying rate of oils if added to the mixture.
Regarding the nature of oil binder, it is possible to confirm that the paint solution does not contain only a drying oil, but it is mixed with another organic binder since A/P ratio is not higher that 1 . Moreover, it can be characterized as mixture of linseed oil and other drying oil which cannot be identified since P/S after 7 months is 1.10, similar to the oil paints investigated previously. Furthermore, A/Sub ratio is 4.13 after 7 months suggesting the use of a pre-heated oil.

Table 24 Concentration (µg/mg) of the main fatty acids present over time in the Solution d'ambre à l'huil de lin mock-up.

FA	Concentration over time (µg/mg)								
	0h	48h	1w	2w	4w	2m	4m	6m	7m

Oleic acid	29.52	44.52	33.52	29.36	26.28	22.17	16.54	11.28	13.42
Linoleic acid	20.53	19.12	2.94	0.90	0.27	0.45	0.35	0.78	0.44
Linolenic acid	6.62	6.39	2.51	3.50	2.26	2.09	2.84	3.27	3.68
Suberic acid	0.18	0.35	1.70	1.20	1.23	2.35	2.76	3.22	4.06
Azelaic acid	3.39	7.51	11.25	9.42	10.60	12.09	12.79	14.33	16.80
Sebacic acid	0.00	0.00	1.06	0.97	0.86	1.08	1.30	1.40	1.79

Table 25 Molar ratios of some fatty acids and %D changing over time in the Solution d'ambre à l'huil de lin mock-up.

Molar ratios	**Molar ratios and %D over time**								
	0h	**48h**	**1w**	**2w**	**4w**	**2m**	**4m**	**6m**	**7m**
A/P	0.15	0.37	0.60	0.53	0.66	0.77	0.92	1.04	0.97
D/P	0.16	0.39	0.74	0.65	0.79	0.99	1.21	1.37	1.31
O/S	1.86	2.77	2.19	1.82	1.89	1.61	1.32	0.83	0.86
%D	3.57	5.72	13.54	12.64	16.04	19.43	22.75	29.04	26.06

3.1.1.2. Solution à peindre 25 ml

According to the Blockx company, the *Solution à peindre 25 ml* is composed of pure amber, aspic essence (or spike oil), poppy oil, and turpentine. The ATR-FTIR spectrum (Error! Reference source not found.) shows the main absorptions of a drying oil as reported in **Table A1**, as the carbonyl peak at 742 cm^{-1} and the peaks at 2852, 2922 and 2953 cm^{-1} attributed to the stretching vibration of CH_2/CH_3 stretching vibrations. As mentioned before, these peaks are typical also for natural resins, so the identification of a resin is quite difficult even if a band at 2676 cm^{-1} which is associated to the O-H stretching of a dimerized carboxyl group can be observed [78], [79].

In addition, some peaks which can be attributed to turpentine are also present. In particular, 786, 886, 1017, 1052, 1099 and 2730 cm^{-1} [80], [81].

Regarding the drying process, the percentage weight variation curve is shown in Error! Reference source not found.. It shows a little weight loss (-1%) in the first three hours followed by a weight gain (2%) due to the oxygen uptake. Then within 24 hours a weight loss (-3%) occurs. Other weight fluctuations can be observed during the third day of ageing and after that the curve appears stable suggesting that the film polymerization is occurring.

The FTIR-ATR spectra reported in Error! Reference source not found. show the characteristic changes in molecular composition which occur over time during the film formation. It is fundamental the decrease of the small peak at 3006 cm^{-1} already after 24 hours suggesting the involvement of the unsaturated fatty acids in the oxidation process. This peak totally disappears within the first week. The carbonyl peak at 1742 cm^{-1} becomes wider already after 24 hours

with the formation of degradation products such as aldehydes and ketones by the hydrolysis of triglycerides. In addition, the intensity of the peak at 1163 cm^{-1} related to the C-O stretching of esters increases within the first 24 hours becoming more visible after 1 week. .

Nevertheless, it is possible to notice an unusual increase over time of the peak at 722 cm^{-1} which is attributed to the bending modes of the C=C-H unsaturated bonds of UFAs. This phenomenon occurs in the infrared spectra of all three painting solutions. Since the peak at 3006 cm^{-1} decreases suggesting that the oxidation reaction is occurring, the increase in intensity of the peak at 722 cm^{-1} can only be explained as the cause of the influence of the Melinex® sheet on which the oil film was applied. It is in fact a polyethylene terephthalate (PET) film which shows its strongest infrared absorption at about 720 cm^{-1} due to the out of plane bending of the benzene group [82]. PET shows also a very strong peak at about 1730 cm^{-1} due to carbonyl stretching which is added to the carbonyl peak of the paint solution, resulting in an increase in intensity over time which is not due to variations of the molecular composition.

The GC-MS analysis allowed to better understand the change in molecular composition during film formation. In Error! Reference source not found., the two chromatograms acquired at 0 hours and after 7 months are reported. The latter shows several compounds such as fatty acids with a lower molecular weight, oxidation products in different form like oxo- and hydroxy-, and dicarboxylic acids. In particular, oxidation products appear already within the first week.

The molecular composition of oil film changes consistently within the first week (**Table 26**). In fact, it is possible to observe a strong increase of dicarboxylic acids, especially azelaic acid.

The decrease of unsaturated fatty acids can be also observed. Oleic acid decreases slowly over time, while linoleic acid decreases until it disappears after 4 months.

By observing the molar ratios in **Table 27**, it is possible to notice a general increase over time of A/P, D/P and %D, except O/S due to the increase of dicarboxylic acids in the oil composition. Also in this case, as for *Solution d'ambre à l'huil de lin,* O/S ratio does not reach the value between 0.1 and 0.2 suggesting that the drying process is still occurring. The presence of a resin in the formulation can have this slowing effect.

Table 26 Concentration (µg/mg) of the main fatty acids present over time in the Solution à peindre 25 ml mock-up.

FA	Concentration over time (µg/mg)								
	0h	48h	1w	2w	4w	2m	4m	6m	7m

Oleic acid	35.85	38.62	34.33	30.35	22.70	11.60	4.34	4.86	3.59
Linoleic acid	40.53	42.81	11.99	1.96	0.86	0.17	0.00	0.00	0.00
Linolenic acid	3.12	0.90	1.70	2.60	1.34	1.83	1.68	2.14	2.20
Suberic acid	0.00	0.00	0.62	0.50	1.12	2.43	3.78	4.97	5.35
Azelaic acid	0.42	0.24	8.03	5.68	7.80	10.70	12.69	15.33	15.95
Sebacic acid	0.00	0.00	1.23	1.10	0.90	1.50	2.11	2.67	2.62

Table 27 Molar ratios of some fatty acids and %D changing over time in the Solution à peindre 25 ml mock-up.

Molar ratios	**Molar ratios and %D over time**								
	0h	**48h**	**1w**	**2w**	**4w**	**2m**	**4m**	**6m**	**7m**
A/P	0.03	0.01	0.50	0.40	0.55	0.84	1.04	1.15	1.01
D/P	0.03	0.01	0,62	0.51	0.70	1.15	1.52	1.72	1.52
O/S	3.07	2.77	2.88	2.55	2.08	1.17	0.43	0.43	0.29
%D	0.36	0.17	9.28	9.30	14.39	24.20	32.94	39.22	33.58

3.1.1.3. Solution à peindre 10 ml

According to the Blockx company, the *Solution à peindre 10 mL* has the same composition of the *Solution à peindre 25 mL* with a surplus of turpentine (70% solution à peindre and 30% turpentine). In fact, the main absorptions of drying oil are present in the ATR-FTIR spectrum (Error! Reference source not found.) and in general the spectral shape is very similar to the one of *Solution à peindre 25 ml*. Nevertheless, it is possible to notice that the peak at about 3008 cm^{-1} is not present, suggesting that the drying oil contained is not fresh. In fact, already before the preparation of the mock-ups, the paint solution was dense and darker than normal, due to a first oxidation. It is possible that the container was not well sealed and that the drying of the oil began slowly.

The graphical representation of percentage weight variation appears very instable in the first three days then it does not show any other weight fluctuations from the third week.

ATR-FTIR spectra acquired during the 7 months monitoring period does not show characteristic variations in spectral absorptions, due to the fact that this paint solution had already undergone a partial oxidation polymerization before the application and in addition, the influence of Melinex® film makes both peaks at 1736 and 720 cm^{-1} increasing, as already seen for the other two paint solutions.

GC-MS analysis shows some characteristic change in oil composition over time. In fact, by observing the two chromatograms acquired at 0 hours and 7 months it is possible to notice the presence of other compounds like oxidation products after 7 months suggesting that an oxidation and polymerization process have occurred (Error! Reference source not found.).

The molecular composition of oil film changes over time showing some inconstant values of unsaturated fatty acids especially in the first month (**Table 28**). This phenomenon is probably due to the fact that the consistency of the solution has not allowed the perfect layering on the Melinex® film probably creating regions ticker than others and therefore at different stages of the drying process.

However, by observing the molar ratios reported in **Table 29**, it is possible to notice a general increase over time of A/P, D/P and %D.

Table 28 Concentration (µg/mg) of the main fatty acids present over time in the Solution à peindre 10 ml mock-up.

FA	Concentration over time (µg/mg)								
	0h	48h	1w	2w	4w	2m	4m	6m	7m
Oleic acid	33.22	38.55	40.64	34.67	39.08	21.86	11.17	7.55	4.04
Linoleic acid	4.01	7.51	4.84	2.92	6.07	0.73	0.50	0.02	1.85
Linolenic acid	1.84	2.72	2.06	1.52	2.11	0.97	1.71	2.32	1.21
Suberic acid	0.00	0.00	0.00	0.00	0.18	0.62	1.17	1.52	1.77
Azelaic acid	0.30	0.80	0.58	0.68	1.98	2.05	2.53	3.04	3.41
Sebacic acid	0.00	0.00	1.39	1.31	3.88	2.01	2.47	2.52	2.54

Table 29 Molar ratios of some fatty acids and %D changing over time in the Solution à peindre 10 ml mock-up.

Molar ratios	Molar ratios over time (%)								
	0h	48h	1w	2w	4w	2m	4m	6m	7m
A/P	0.03	0.06	0.05	0.06	0.06	0.19	0.25	0.30	0.31
D/P	0.03	0.06	0.17	0.19	0.19	0.44	0.60	0.69	0.70
O/S	3.65	3.14	3.41	3.15	1.31	2.33	1.32	0.85	0.44
%D	0.47	0.96	2.49	2.97	4.53	8.84	14.70	18.46	19.28

3.1.2. Blockx oil paint mock-ups set2

In this paragraph the study over time of three oil paint by Blockx (*Blanc de Titane*, *Bleu de Cobalt,* and *Vert de Cobalt*) mixed with the *Solution à peindre 25 ml* is presented. The study has been carried out by means of ATR-FTIR, GC-MS analysis and the calculation of percentage weight variation.

3.1.2.1. Blanc de Titane + Solution à peindre 25 ml

The mixture *Blanc de Titane + Solution à peindre 25 ml* shows a weight loss of about 1% in the first three hours followed by a period of stability until a weight gain of up to 1% during the third day probably due to the oxygen uptake (Error! Reference source not found.). Then another weight loss within the first week and after that the curve appears stable until the end of the monitoring period of 5 months. The first weight loss can be attributed to the evaporation of volatile terpene fraction since turpentine and the essential oil aspic essence.
The ATR-FTIR spectra reported in Error! Reference source not found. show the main spectral variations within 72 hours. The small peak at 3011 cm^{-1} decreases as early 24 hours and it is no longer visible in the 1 week infrared spectrum, suggesting that the oxidation phase is occurred. In addition, the carbonyl peak at 1744 cm^{-1} decreases in intensity overtime and becomes broader due to the hydrolysis of triglycerides and the formation of degradation products as aldehydes, ketones, and free fatty acids. After 1 week also a band at about 1600 cm^{-1} is visible and it increases over time until 5 months. It is formed by the increase of intensity of two peaks at about 1650 and 1570 cm^{-1} attributed to the COO- bending of fatty acids.
The variation of the molecular composition over time has been observed and studied also by means of GC-MS. In Error! Reference source not found.Error! Reference source not found., the two chromatograms at 0 hours and after 7 months are reported. Comparing them, it is possible to notice the significant increase of dicarboxylic acids at the expense of unsaturated fatty acids, but also the formation of new products like oxidation products in different forms and the consequential transformation of the oil composition no longer composed only of triglycerides and free fatty acids.

The quantitative analysis shows that the strong decrease of unsaturated fatty acids in favour of dicarboxylic acids occurs within the first week, since in the chromatogram after 48 hours only slight variation can be noticed (**Table 30**).

In particular, there is a strong decrease of oleic acid and a slow increase of dicarboxylic acids, especially of azelaic acid. A little amount of azelaic acid is always present at 0 hours, due to the fact that the painting products used for this study are not sealed but already open.
Considering the molar ratios reported in **Table 31**, it is possible to notice a general increase over time of A/P, D/P and %D due to the increase of dicarboxylic acids in the oil composition and a decrease of O/S. In fact, O/S ratio indicates the maturity of the drying oil since the unsaturated acid (oleic acid) is particularly reactive to oxygen when oil film is exposed to air. In this case, as for the paint solutions previous investigated, the O/S ratio does not reach the 0.1-0.2 value suggesting that oxidation process is still slowly occurring. In fact, D/P ratio and %D continue to increase until seven months after a strong increase within the first week showing that the polymerization of the film is still taking place.

Table 30 Concentration (µg/mg) of the main fatty acids present over time in the Blanc de Titane + Solution à peindre 25 ml mock-up.

FA	Concentration over time (µg/mg)								
	0h	48h	1w	2w	3w	4w	2m	3m	5m
Oleic acid	35.68	25.34	7.06	6.14	4.56	5.85	3.42	2.91	2.39
Linoleic acid	20.83	23.08	11.08	0.20	0.24	0.14	0.12	0.17	0.11
Linolenic acid	2.10	1.49	2.33	2.11	1.54	1.42	1.71	1.32	1.39
Suberic acid	0.00	0.00	1.17	1.06	1.45	2.84	2.31	2.42	3.52
Azelaic acid	0.28	2.42	8.08	9.74	9.21	12.38	9.56	9.79	13.72
Sebacic acid	0.00	0.19	0.39	0.52	0.58	1.15	0.87	0.92	1.30

Table 31 Molar ratios of some fatty acids and %D changing over time in the Blanc de Titane + Solution à peindre 25 ml mock-up.

Molar ratios	Molar ratios and %D over time								
	0h	48h	1w	2w	3w	4w	2m	3m	5m
A/P	0.03	0.19	0.68	0.92	0.93	1.01	1.09	1.03	1.08
D/P	0.03	0.21	0.81	1.07	1.13	1.34	1.46	1.38	1.46
O/S	5.22	3.42	1.05	1.83	0.84	0.79	0.60	0.49	0.32
%D	0.33	3.17	17.08	25.83	32.03	30.92	32.56	32.76	37.06

3.1.2.2. Bleu de Cobalt + Solution à peindre 25 ml

The curve of the percentage weight variation of the mixture *Bleu de Cobalt + Solution à peindre 25 ml* shows the weight loss in the first three hours already seen in the previous mixture suggesting that it may be a characteristic of terpenoids drying process (Error! Reference source

not found.). Then during the first and the second day a little instability can be observed until a weight gain of about 1,50% at 72 hours followed by a weight loss (up to 1%) at 1 week. From 2 weeks, the drying curve appears very stable.

The ATR-FTIR spectra acquired during the 5 months of monitoring show some changes in the molecular composition of the mixture within 48 hours (Error! Reference source not found.). Indeed, the small peak at 3013 cm^{-1} decreases until it disappears after 72 hours; the carbonyl peak at 1743 cm^{-1} becomes broader, the intensity of the band at about 3400 cm^{-1} increases as early 24 hours and it increases over time until 5 months. In addition, the peak at 1625 cm^{-1} increases over time in intensity almost covering the one at 1575 cm^{-1}. Already after 72 hours some stability can be observed

Figure 3 GC-MS chromatograms of *Bleu de Cobalt + Solution à peindre 25 ml* after 0 hours (left) and after 5 months (right)

The two chromatograms at 0 hours and 7 months are reported in **Figure 3**. The latter appears more complex than the one at 0 hours because of several new products like oxidation products in different forms are present.

The quantitative analysis shows that the strong decrease of unsaturated fatty acids in favour of dicarboxylic acids occurs within the first week, as observed in the mixture previously investigated (**Table 32**). Similarly, to the previous mixture, there is a strong decrease of oleic acid and a slow increase of dicarboxylic acids, especially of azelaic acid.

Considering the molar ratios reported in **Table 33**, it is possible to notice a general increase over time of A/P, D/P and %D due to the increase of dicarboxylic acids in the oil composition and a constant decrease of O/S from the first week. Moreover, the O/S ratio does not reach the 0.1-0.2 value suggesting that oxidation process is still slowly occurring. In fact, as seen before, D/P ratio and %D continue to increase until seven months after a strong increase within the first week showing that the polymerization of the film is still taking place.

Table 32 Concentration (µg/mg) of the main fatty acids present over time in the Bleu de Cobalt + Solution à peindre 25 ml mock-up.

FA	Concentration over time (µg/mg)								
	0h	48h	1w	2w	3w	4w	2m	3m	5m
Oleic acid	46.93	30.21	12.56	9.53	6.09	7.06	5.14	4.14	4.00
Linoleic acid	33.21	14.12	2.72	1.83	0.24	0.09	0.07	0.13	0.12
Linolenic acid	8.27	1.56	1.85	2.05	1.99	1.37	1.76	1.39	2.93
Suberic acid	0.00	0.00	1.21	1.59	1.54	3.84	2.71	3.03	4.81
Azelaic acid	0.28	5.40	9.39	10.58	11.10	15.81	11.40	11.81	18.54

Sebacic acid	0.09	0.14	0.66	0.91	0.71	1.74	1.22	1.34	1.98

Table 33 Molar ratios of some fatty acids and %D changing over time in the Bleu de Cobalt + Solution à peindre 25 ml mock-up.

Molar ratios	**Molar ratios and %D over time**								
	0h	**48h**	**1w**	**2w**	**3w**	**4w**	**2m**	**3m**	**5m**
A/P	0.02	0.42	0.83	0.94	1.06	1.23	1.25	1.27	1.27
D/P	0.03	0.43	0.99	1.16	.28	1.66	1.68	1,74	1.74
O/S	3.98	2.79	0.27	0.19	0.62	0.59	0.58	0.47	0.30
%D	0.29	6.35	19.43	23.29	29.20	32.36	32.34	33.86	35.88

3.1.2.3. Vert de Cobalt + Solution à peindre 25 ml

The curve of the percentage weight variation of the mixture *Vert de Cobalt + Solution à peindre 25 ml* shows a little weight loss in the first three hours already seen in both previous mixtures (Error! Reference source not found.). Then during the first and the second day a little instability can be observed until a weight gain of more than 1,50% at 72 hours followed by a weight loss (almost 1,50%) at 78 hours. After 2 weeks, the drying curve appears very stable.
The ATR-FTIR spectra acquired during the 5 months of monitoring show some changes in the molecular composition of the mixture within 48 hours (Error! Reference source not found.). Indeed, the small peak at 3008 cm^{-1} decreases until it disappears after 48 hours showing a fast drying rate also due to the cobalt and zinc ions present in the green pigment. Furthermore, the carbonyl peak at 1745 cm^{-1} becomes broader within 48 hours, the intensity of the band at about 3400 cm^{-1} increases as early 24 hours and it increases over time until 1 week. In addition, the band at 1625 cm^{-1} appears within 24 hours and it increases until 5 months. Already after 48 hours some stability can be observed

The quantitative analysis shows that the strong decrease of unsaturated fatty acids in favour of dicarboxylic acids occurs within the first week, since in the chromatogram after 48 hours only slight variation can be noticed (**Table 34**).
In particular, as seen before there is a strong decrease of oleic acid within 48 hours until it almost disappears completely and an increase of dicarboxylic acids , especially of azelaic acid. Considering the molar ratios reported in **Table 35**, it is possible to notice a general increase over time of A/P, D/P and %D and a decrease of O/S. After 5 months, D/P ratio and %D seems to stabilize suggesting that the polymerization of the film is almost occurred.

Table 34 Concentration (µg/mg) of the main fatty acids present over time in the Vert de Cobalt + Solution à peindre 25 ml mock-up.

FA	Concentration over time (µg/mg)								
	0h	48h	1w	2w	3w	4w	2m	3m	5m
Oleic acid	18.04	2.75	3.59	1.04	1.65	1.54	1.48	1.08	1.52
Linoleic acid	30.73	10.04	2.28	2.23	0.12	0.10	0.14	00.7	0.14
Linolenic acid	1.71	0.97	0.91	1.05	0.94	0.75	0.72	0.66	0.81
Suberic acid	0.00	0.45	1.53	1.99	1.64	3.55	2.56	2.44	3.72
Azelaic acid	0.22	4.99	7.94	9.01	8.37	13.06	9.68	8.94	12.82
Sebacic acid	0.08	0.29	0.48	0.58	0.49	0.99	0.76	0.71	1.06

Table 35 Molar ratios (%) of some fatty acids changing over time in the Vert de Cobalt + Solution à peindre 25 ml mock-up.

Molar ratios	Molar ratios over time (%)								
	0h	48h	1w	2w	3w	4w	2m	3m	5m
A/P	0.02	0.55	0.90	0.98	1.02	1.08	1.06	1.08	1.14
D/P	0.03	0.63	1.12	1.84	1.28	1.46	1.43	1.46	1.57
O/S	3.28	0.54	0.70	4.53	0.40	0.25	0.30	0.24	0.25
%D	0.43	14.13	29.42	33.21	38.37	39.01	38.03	38.64	40.85

3.2. Comparison of behaviour over time of set1 and set2

According to the results just presented, the drying process of a lipid binder can be influenced by different factors which can be internal or external the oil formulation itself. Blockx oil paints show a similar drying behaviour which consists in a weight gain in the first hours due to oxygen uptake by UFAs present in the oil composition and then a weight loss due to the evaporation of volatile compounds formed during the drying process. The weight loss always occurs within the first day after the application of the film, nevertheless the achievement of a weight stability varies depending on the oil paint. In fact, it was possible to observe that oil paints which contains cobalt-based pigments like *Bleu Coeruleum*, *Bleu de Cobalt* and *Vert de Cobalt*, they reach some stability which also means any other changes in the infrared spectral curve and a little and constant variation of A/P, D/P, and %D as early 24/48 hours. Among these, *Vert de Cobalt* is the color that first reaches stability and this is explained by the presence of cobalt (primary drier) that is zinc (auxiliary drier) in its formulation.

Regarding the mixture of *Blanc de* Titane, *Bleu de Cobalt,* and *Vert de Cobalt* with *Solution à peindre 25* ml, a typical weight loss in the first three hours has been observed probably attributed to the evaporation of terpenoids present in turpentine and aspic essence.

Nevertheless, even if they show many weight fluctuations during the drying process, considering the molar ratios %D and O/S, any particular differences in drying rate have been observed, even if it was expected. It is probably due to the low amount of *Solution à peindre 25 ml* in the 1:5 ratio of amber and oil. Moreover, also the presence of turpentine in the formulation of the paint solution may have influenced the drying rate by speeding it. Therefore, it is possible to affirm that this particular ratio of amber and oil does not change the typical behaviour of the oil paint, but it permits to improve the viscosity of oils for glazing technique, which was the main reason why in the beginning the Flemish masters added it to the lipid binder.

3.3. Identification of markers related to the Blockx production: focus on liquid amber and spike oil

The characterization of the Blockx painting solutions, has allowed to confirm the presence of Baltic amber as main component in addition to the lipid binder. By means of py-GC-MS, some marker of Baltic amber has been found, in the terpenic fraction of the three painting solutions. In addition to succinic acid, which is the main marker of Baltic amber, other compounds which can be associated to the Baltic amber have been found. They are:

- Tricyclo[20.8.0.0(7,16)]triacontane, 1(22),7(16)-diepoxy-
- 2-[4-methyl-6-(2,6,6-trimethylcyclohex-1- enyl)hexa-1,3,5-trienyl]cyclo
- 2-[5-(2,2-Dimethyl-6-methylene-cyclohexyl)-3-methyl-pent-2-enyl]-[1,4]benzoquinone.

These compounds have been found in archaeological Baltic amber samples.

4. Case study

4.1. The temptation of Saint Anthony by Salvador Dalí (1946)

The case study selected for this thesis project is the work of art *The temptation of Saint Anthony* made by the Spanish surrealist painter Salvador Dalí in 1946 and housed at the Royal Museum of Fine Arts of Belgium, in Brussels (Error! Reference source not found.). It is an oil painting on canvas made for a contest on the theme of the temptation of St. Anthony held by the American film producer Albert Lewin, to be used in the film *The Private Affairs of Bel Ami*, to

which twelve surrealist and avant-garde painters of the time participated, including Max Ernst, who received the first prize. The theme of the Temptation of Saint Anthony has been long represented by artists and authors in their art. It is based on the life of Anthony the Great who suffered the temptations of the Devil to which he was able to resist during his retreat in the desert as a hermit [83].

"The temptation of Saint Anthony" by Salvador Dalí depicts indeed the battle between the good and the evil in a desertscape with a low horizon line and a light-blue sky darkened in the background by black clouds. In the bottom left corner, Dalí painted the figure of the saint on his knees who holds up a cross in his right hand against the evil represented as a parade of elephants carrying symbolic objects representing temptation and led by a horse, depiction of Satan.

As already mentioned, this painting has been studied in the frame of the *Face to Face* project by David Strivay and Catherine Defeyt from the CEA of the University of Liège during two analytical campaigns between 2019 and 2020 and it was the subject of the study of the master thesis "Analyse par spectroscopies vibrationnelles et fluorescence des rayons X de l'œuvre « La Tentation de Saint-Antoine » de Salvador Dalí » by Soline Hardy [2].

All the previous analyses have been carried out *in situ* by means of infrared and Raman spectroscopy, and XRF spectrometry. This study particularly focused on the characterization of the inorganic materials (mostly pigments) present in the work of art. ATR-FTIR analysis showed the presence of a lipidic binder, but it has not been uniquely identified. So, to better understand the material composition of the Dalí painting and its stratigraphy, in this thesis seven samples have been studied by means of ATR-FTIR, micro-Raman spectroscopy, XRF, SEM-EDS and GC-MS. The samples were collected by prof. David Strivay and Dr. Catherine Defeyt during one of the two analytical campaigns of the work of art at the Royal Museum of Fine Arts of Belgium in 2019. They were taken from the regions of the canvas that presented detachments and from the marginal parts covered by the frame, to make their removal not visible (Error! Reference source not found.). They were named S1-S7 (as sample1-sample7). Just three of them (S4, S5, S6) had already been analyzed only by means of micro-Raman spectroscopy. The results are reported in the master thesis mentioned before and they will be discussed in the following section.

4.2. Previous study of the painting

The areas of the painting analyzed during the previous study by CEA correspond to the figure of St. Anthony, two of the symbolic objects carried on the elephants' back (obelisk and temple), the light-gray clouds in front of the elephant in the background, and an area of the ground in the lower right-hand corner corresponding to Dalí's signature. They were mainly analyzed to investigate the chemical composition of the pigments present on the external pictorial layer. Nevertheless, on the edges of the canvas were also visible the lower layers related to the preparation; thus, it was also possible to hypothesize the chemical composition of the ground layer. The latter has been described as an opaque white layer probably made of lead white. During the campaign of 2019 also anatase and gypsum have been identified. Regarding the main pigments present in the painting, it is possible to mention cobalt green, aureolin, cadmium yellow and a black pigment (ivory black or vine black). Moreover, also fillers and extenders have been identified, like gypsum, barium sulphate and potassium sulphate.

4.3. Sample investigation: study of artist's materials

Based on the results of the previous studies, the present thesis aims to better characterize the material composition and the stratigraphy of this painting and then to investigate the relationship between Salvador Dalí and the products by the Belgian company Blockx which as already mentioned were most probably used by the artist.

As mentioned before, seven samples collected by CEA have been analyzed by means of a multi-analytical approach. In **Table 36** it is possible to observe the photos under optical microscope and the description of the samples. As reported, S1, S2 and S5 have been taken from the upper edge of the canvas, where any pictorial layer can be observed. S1 and S5 consist of a single layer with a yellowish and translucent colour, similar to a resinous material. The back of both samples shows some transparent filaments which can be related to a protein-based material, such as glue, typically used to prepare the canvas prior to painting (sizing)[1]. S2 consists of two layers, including a lower one equal to the one described above and an upper one with a whitish and homogeneous appearance and some dark grains (red and bluish) spread all over the layer. This second layer can be related to the preparation layer, also called ground layer, which usually consists in a protein-based binder mixed with thin chalk.

[1] Sizing layer or simply size is the very first step in the preparation of the painting support. It is a layer (usually of glue) that penetrates into the pores of the fibers, sealing them to isolate the support from direct contact with the oil paint vehicle.

S3 also consists of two layers, a lower one of ground layer and an upper one of dark-gray pictorial layer. S4, S6 and S7 consist of single pictorial layer. As reported in **Table 36**, S4 and S7 have been taken from a colour dripping respectively from the bottom and the left edge, but as it is possible to observe in **Error! Reference source not found.**, they both correspond to the dark-gray pictorial layer of the ground. S6 has been taken instead from a light-gray cloud in the middle of the painting, and in particular from an interesting drop of colour.
According to this first description, it is possible to affirm that the samples taken are quite similar because they consisted of no more than two layers, including the sizing, the ground layer and the pictorial layer, in this case of a dark grey/black colour. Then based on the results that will be reported in this study, they could be grouped into three groups related to these three kind of layers.

Table 36 OM pictures and description of the seven samples taken from the "The temptation of Saint Anthony" by Salvador Dalí and analyzed in this study.

4.3.1. Inorganic component: pigments and additives

To first characterize the inorganic fraction of these samples, elemental analyses by means XRF and SEM-EDX have been carried out.
XRF measurement have been performed on six samples. S4 was not analyzed because it appears to be composed of very small grains, of powdery consistency.
The main elements found on almost all samples are calcium, sulphur, titanium, zinc, and small amounts of iron. In addition, in grey samples (S3 and S6) abundance of lead, and traces of copper, manganese and cobalt have been found.
According to XRF measurements, it is possible to affirm that the sizing layer (S1, S2_back, S5) contains calcium as main component, together with sulphur, but also small amounts of zinc, iron, and titanium. The latter is present only in S1 and not in S5; therefore, it may be a residue of the upper layer (ground layer). Indeed, the upper layer of S2 (white layer) is mainly composed of calcium and sulphur, but also titanium (Error! Reference source not found.**a**), suggesting the presence of gypsum ($CaSO_4 \cdot 2H_2O$) and titanium white (TiO_2),
The spectrum of S3 front (gray layer) shows high percentage of lead, followed by calcium and sulphate, which together with small amount of titanium can be related to the lower layer, since the pictorial layer appear to be very thin. In addition, iron, manganese, and copper have been detected, even if it is not possible to confirm their presence with certainty, due to their errors (Error! Reference source not found.**b**). S6 contains also high amounts of lead followed by

sulphur, but small amount of calcium and no presence of titanium, supporting the hypothesis that calcium and titanium are related to the preparation layer that in this case is not presence (Error! Reference source not found.**c**). Instead, the presence of lead can be related to cerussite and massicot already identified by means of Raman spectroscopy during the previous study of the painting [2].

S7 is instead a sample a bit different compared to the others. As mentioned before in **Table 36**, it was sampled from a colour dripping on the left edge of the canvas and it contains mainly calcium and iron, but also zinc and unlikely titanium, as shown in Error! Reference source not found.**d**.

Two samples S2 and S3 have been also embedded in resin to investigate their cross-section given their interesting stratigraphy (Error! Reference source not found.). Indeed, they are the only ones to present two layers, consisting of preparation layers (sizing and ground layer) in S2 and pictorial layer and ground layer in S3. They have been observed under OM and analyzed by means of SEM-EDX which allowed to observe both the morphology of the stratigraphy (BEI images) and to characterize the elemental composition of the single layers thanks to the EDX mapping. The regions investigated are the areas within the dotted line in Error! Reference source not found..

The white ground layer (layer II) present in S2 and S3 has a thickness of 100 µm and appears very compact and consistent with some orange-pink lamellar grains and some darker ones. Instead, the yellow sizing (I layer) is a very incoherent layer of 100 µm thickness with many voids since most probably the material of which it is composed has not withstood the mechanical heat of simple lapping with sandpaper. Regarding the pictorial layer (III layer) of S3, by observing the BEI image (Error! Reference source not found.) it appears very thin but compact and homogeneous. It has a thickness of about 40 µm.

EDX mapping of S2 (Error! Reference source not found.) shows that ground layer (upper) is mainly composed of calcium, sulphur, and titanium, supporting the results of XRF analysis. Therefore, it is possible to hypothesize the use of gypsum and titanium white to make the preparation layer usually mixed with a protein-based binder and oil [84]. Furthermore, in the same ground layer it is also possible to observe the presence of silicon and magnesium in the areas corresponding to those orange-pink lamellar grains spread all over the layer, suggesting the presence of talc ($Mg_3Si_4O_{10}(OH)_2$, magnesium silicate hydrate) which is a clay mineral usually used as a filler in modern paint formulations [85]. It can be easily confirmed because the orange-pink colour observed by means of the optical microscope is one of the typical colour of talc as white, green, gray, brown etc.

In S3 cross-section (Error! Reference source not found.) the ground layer is mainly composed by calcium, sulphur and titanium with lamellar grains made of silicon and magnesium confirming the same composition of the II layer of S2. Moreover, the EDX mapping shows that the pictorial layer in S3 is mainly composed of lead and sulphur, and probably of phosphate. These elements can suggest the use of a lead-based pigment which can correspond to lead white or cerussite ($PbCO_3$) that was found on S4 by means of Raman spectroscopy during previous study [2]. According to a hypothesis suggested by CEA, phosphate can be related instead to the presence of a black pigment such as ivory black which is mainly composed of calcium phosphate, but also carbon and calcium carbonate.

Some punctual analyses have been also performed on the same areas of EDX mapping confirming the presence of the main elements and introducing other ones. In particular, in S2 cross-section the presence of talc has been confirmed by precisely analyzing a lamellar grain of it; indeed, it mainly shows silicon and magnesium (as shown in spectrum (d) in Error! Reference source not found., Error! Reference source not found.). Also, sodium and potassium have been detected both on S2 (point c) and S3 (point d, Error! Reference source not found.). In addition, in S3 also abundance of aluminum has been found indicating

the presence of feldspars (such as ($(Na, K)AlSi_3O_8$)), which are the main components in clay bodies. This can be related to the use of clay as extender/filler in paint formulations [85].

ATR and micro-Raman spectroscopy have been then performed to confirm the presence of the inorganic components and to hypothesize the organic ones, prior to analyze them by means of GC-MS.

By means of ATR analysis it was possible to clearly distinguish the three investigated layers: sizing, ground layer, and pictorial layer (Error! Reference source not found.).

ATR spectra of S1, S2_back (layer I) and S5 are very similar corresponding to the sizing layer. They show the characteristic peaks of a protein-based binder, and in particular animal glue. In S1 (**Figure 4**) the stretching vibration of C=O (amide I) is at 1643 cm^{-1}, the in plane bending vibration of N-H (amide II) at 1538 cm^{-1}, and the C-N stretching vibrations at 1453 cm^{-1}. The presence of a protein-based material is also confirmed by the broad band at 3304 cm^{-1} and the weak one at 3079 cm^{-1} related to the N-H stretching [86], [87]. Other minor peaks are at 1411, 1337, 1235, 1038 and 656 cm^{-1}. Moreover, the peaks at 2922, 2854, 1377, 1159 cm^{-1} may be related to the presence of a lipid material like a drying oil [64], [65].

The Raman spectrum shows peaks at 3063 cm^{-1}, and symmetric and asymmetric stretching of CH_3 respectively at 2875 and 2927 cm^{-1} which can associated to a proteinaceous-based glue (Error! Reference source not found.) [88].

Regarding the inorganic components, mainly calcite ($CaCO_3$), and anhydrite ($CaSO_4$, phase of $CaSO_4$-H_2O system) have been identified. Calcite shows its characteristic peaks at 710 and 873 cm^{-1} in infrared spectrum [89] and it is clearly visible also in Raman spectrum at 1087, 713, 284 and 158 cm^{-1} due to different symmetric stretching modes of CO_3 [70], [89].

The presence of anhydrite in sizing layer has been attested only by means of infrared spectroscopy, suggesting that it may be a residue of the upper ground layer.

In fact, S2 shows very strong peaks related to anhydrite at 1090 cm^{-1} for the antisymmetric stretching vibration modes of SO_4 tetrahedra and at 669, 607 and 590 cm^{-1} corresponding to three antisymmetric bending vibrations (Error! Reference source not found.) [90].

Anhydrite is also clearly visible in the Raman spectrum due to the strong peak at 1017 cm^{-1} and other medium peaks at 1158, 1129, 678, 638, 611, 497 and 417 cm^{-1} due to stretching vibration modes of SO_4 (Error! Reference source not found.) [70], [91], [92].

Moreover, also titanium oxide in anatase form and calcite have been characterized mainly by

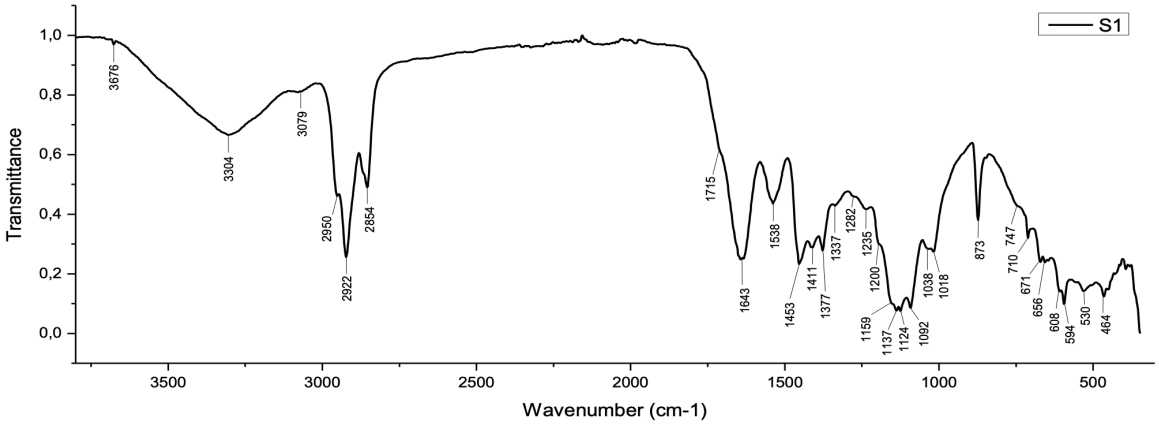

Figure 4 ATR-FTIR spectrum of sample S1.

means of Raman spectroscopy. Anatase shows a very strong peak at 143 cm^{-1} and 193, 394, 513 and 636 (Error! Reference source not found.) [70]. In infrared spectrum only peaks at 1634 related to OH group and 514 cm^{-1} corresponding to Ti-O-Ti bond are visible, due to the presence of strong anhydrite peaks in the region of 700-500 cm^{-1} [93].

In this layer, talc has been also identified, as seen before by means of SEM-EDX. IR spectrum shows a band at 3676 cm^{-1} ascribed to the vibrations of hydroxyl groups Mg (Mg- OH) [94]; the band at 3441 related to Si (Si-OH) may be covered by the 3400 cm-1 broad band attributed to presence of drying oil. Moreover, a band at 1040 cm^{-1} and a shoulder at 677 cm^{-1} correspond to the siloxane group (Si-O-Si) stretching vibration and the Si-O-Mg bond, respectively [30].

As mentioned before, the presence of drying oil can be hypothesized due to the broad band at 3400 cm^{-1} attributed to the stretching vibrations characteristic of the alcohol and hydroperoxide groups resulting from film polymerization and ageing processes. Moreover, bands at 2954,

2922 and 2853 cm^{-1} attributed to the stretching vibrations of the CH_2 and CH_3 groups of fattyacids, the shoulder at 1736 due to C=O stretching vibration, and other peaks at 1456, 1413, The spectrum shows a strong peak at 1708 cm^{-1} which can be attributed to the presence of free fatty acids since the acidic carbonyl (C-O) stretching vibration is generally observed around 1710-1700 cm^{-1} [95]. Furthermore, it is possible to observe the characteristic absorption of metal soaps at 1532 cm^{-1} which corresponds to the antisymmetric stretching vibration of COO- of the carboxylate [95]. It can be associated to a zinc based metal soap [38], [74].

Regarding the samples S3, S6 and S7, they are very similar, even if the IR spectrum of S7 shows some differences. The infrared spectrum of S6 (Error! Reference source not found.), as the S3 spectrum, shows the characteristic peaks of basic lead carbonate ($(PbCO_3)_2 \cdot Pb(OH)_2$), known also as lead white. It exhibits a very strong absorption at 1393 cm^{-1} and a sharp peak at 1045 cm^{-1} attributed to the asymmetric and symmetric stretching of CO_3^{2-} and the typical band at 3529 cm^{-1} attributed to the stretching vibration of OH group [67]. Then, also other bending modes of carbonate group in the region between 900 and 400 cm^{-1} with a maximum at 678, 387 and 358 cm^{-1} are present.

In Raman spectrum (Error! Reference source not found.) it is visible at 57, 75, 104, 414, 679, and 1051 cm^{-1} [70]. Moreover, Raman spectrum shows the characteristic shape of carbon-based material which is more visible in S7 and S3 (Error! Reference source not found.). It consists in two broad bands at about 1330 (D band) and 1600 (G band) cm^{-1} [70].This typical shape is present also in S1 in addition to a weak peak at 2724 cm^{-1} (2D band), suggesting the presence of this black pigment in the sizing layer. In fact, some black grains in the mixture have been observed in this layer under optical microscope.

The ATR-FTIR spectrum of S7 also exhibits the characteristic absorptions of metal soaps at 1598 and 1529 cm^{-1}. They can be associated to a lead and zinc based metal soap, respectively [38], [74].

The organic binder present in this three samples seems to be a drying oil due to the presence of characteristic peaks mentioned above. Nevertheless, it is not possible to clearly identify it. GC-MS has been performed on these sample to characterize the organic fraction.

4.3.2. Organic component: binding media

By means of GC-MS and py-GC-MS it was possible to characterize the organic fraction of the samples. The pictorial medium used by Salvador Dalí is a lipidic binder.

In addition, in sample S3 and S6 which are both composed of pictorial layer, traces of Baltic amber have been detected. Indeed, the characteristic peak of succin acid has been found.

4.4. Conclusions

In conclusion, it is possible to affirm that in this painting three main layers are present: sizing layer, ground layer and pictorial layer. Sizing layer mainly consists of a protein-based material, such as animal glue, mixed with calcite. The presence of anhydrite in this layer may be due to some residue from the upper one, i.e., the ground layer, which consists in anhydrite, titanium oxide and calcite mixed with an organic binder, such as drying oil and probably a natural resin. In addition, talc has been identified, probably present in the formulation of one of this pigment. In fact, it is used as a filler and extender in the paint industry, because of its softness, good diffusion coefficient and low weight.
Regarding paint layer, two kind of layers have been characterized. The black layer consists only of a carbon-based pigment and the gray paint layer from the gray ground of the painting and a cloud results a mix of a carbon-based pigment and lead white.

5. Conclusions

5.1. Characterization of Blockx products

Commercial oil paints by Blockx are oil color mainly composed of linseed oil and inorganic pigment. During drying process, they show a typical behaviour of oil paints mainly influenced by the presence of driers in the paint formulation and

5.2. Comparison of Blockx products and Salvador Dalí pictorial materials

Regarding the relationship between Salvador Dalí and the Belgium company Blockx, it is possible to confirm that Salvador Dalí has used the amber-based painting solution by Blockx. Indeed, the succinic acid (marker of the Baltic amber) has been found in both Blockx painting solutions and two samples taken from Dalí painting. In this regard, the use of amber must relate to the two areas of the painting where the samples were taken. It is not possible to assert that it was used on the whole painting being two samples not representative of the whole work of art.

Future perspectives

Considering the positive results of this research that confirm the relationship between Salvador Dalí and the Belgium company Blockx, it could be interesting to continue this study by considering and analyzing other paintings of the Spanish painter. In this way, it would be possible to better understand this relationship and its duration.

Moreover, to better understand the more volatile fraction of the amber-based painting solutions, it would be necessary to study different methods to analyze them by means of GC-MS and/or py/GC-MS. Indeed, finding the markers of the spike oil would be very interesting since the company Blockx counts it among the main ingredients.

References

[1] S. Dalí, *50 Secrets of magic craftsmanship*. New York: Dial Press, 1948.

[2] S. Hardy, 'Analyse par spectroscopies vibrationnelles et fluorescence des rayons X de l œuvre « La Tentation de Saint-Antoine » de Salvador Dali', Université de Liège, 2021.

[3] G. Vasari, *Le Vite de più eccellentissimi pittori e scultori italiani, da Cimabue insino a' tempi nostri*. Firenze: Torrentino, 1550.

[4] Y. Taniguchi, 'Constituent Material Analysis of the Bamiyan Buddhist Wall Paintings in Central Asia : Organic Analysis Using GC / MS and ELISA', *Bull. Natl. Museum Japanese Hist.*, vol. 177, no. November, p. 2012, 2012.

[5] Y. Taniguchi *et al.*, 'Organic Materials Used for Giant Buddhas and Wall Paintings in Bamiyan, Afghanistan', *Appl. Sci.*, vol. 12, no. 19, 2022, doi: 10.3390/app12199476.

[6] T.-H. Borchert, *Jan Van Eyck*, vol. s6-XII, no. 290. Taschen, 2008.

[7] J. D. J. Van den Berg, 'Analytical chemical studies on traditional oil paints', PhD thesis, Universiteit van Amsterdam, 2002.

[8] F. C. Izzo, P. Ugo, and G. Biscontin, '20th century artists'oil paint : a chemical-physical survey', PhD thesis, University of Ca' Foscari, 2011.

[9] S. Croll, 'Overview of Developments in the Paint Industry since 1930', in *Modern Paints Uncovered*, 2006, pp. 17–29.

[10] M. Pugliese, *Tecnica mista: Materiali e procedimenti nell'arte del XX secolo*. Milano, 2006.

[11] F. C. Izzo, K. J. Van den Berg, H. van Keulen, B. Ferriani, and E. Zendri, 'Modern Oil Paints – Formulations, Organic Additives and Degradation: Some Case Studies', in *Issues in contemporary oil paint*, Springer, 2014.

[12] M. D. Gottsegen, *The Painter's Handbook: Revised and Expanded*. 2006.

[13] R. Mayer, *The artist's handbook of materials and techniques*, 5th ed. New York: Viking, 1991.

[14] M. Matteini and A. Moles, 'La chimica nel restauro. I materiali dell'arte pittorica'. Nardini editore, Firenze, pp. 23–88, 2010.

[15] A. Burnstock, K. J. van den Berg, S. de Groot, and L. Wijnberg, 'An investigation of water-sensitive oil paints ni twentieth-century paintings', in *Modern Paints Uncovered*, 2006, pp. 177–188.

[16] T. J. Learner, 'Analysis of Modern Paints', in *Research in conservation*, 2004, doi:

10.1179/sic.2006.51.3.233.

[17] M. Lazzari and O. Chiantore, ‘Drying and oxidative degradation of linseed oil’, *Polym. Degrad. Stab.*, vol. 65, no. 2, pp. 303–313, 1999, doi: 10.1016/S0141-3910(99)00020-8.

[18] J. S. Mills and R. White, *Organic Chemistry of Museum Objects*, 2nd editio. New York: Routledge Taylor & Francis Group, 1994.

[19] N. O. V. Sonntag, ‘Structure and composition of fats and oils: components affecting the stability of fats and oils’, *Bayley’s Ind. oil fat Prod.*, vol. I, pp. 289–477, 1979.

[20] H. A. L. Standeven, *House Paints, 1900-1960. History and Use*, no. 2. Los Angeles, 2011.

[21] H. Wexler, ‘Polymerization of drying oils’, *Chem. Rev.*, vol. 64, no. 6, pp. 591–611, 1964, doi: 10.1021/cr60232a001.

[22] D. Erhardt, C. S. Tumosa, and M. F. Mecklenburg, ‘Long-term chemical and physical processes in oil paint films’, *Stud. Conserv.*, vol. 50, no. 2, pp. 143–150, 2005, doi: 10.1179/sic.2005.50.2.143.

[23] C. S. Tumosa and M. F. Meckelnburg, ‘Weight changes on oxidation of drying and semi-drying oils’, *Collect. Forum*, vol. 18, no. 1–2, pp. 116–123, 2003.

[24] P. Fjällström, B. Andersson, C. Nilsson, and K. Andersson, ‘Drying of linseed oil paints: A laboratory study of aldehyde emissions’, *Ind. Crops Prod.*, vol. 16, no. 3, pp. 173–184, 2002, doi: 10.1016/S0926-6690(02)00035-3.

[25] C. S. Tumosa and M. F. Mecklenburg, ‘Oil Paints: The Chemistry of Drying Oils and the Potential for Solvent Disruption’, *New Insights into Clean. Paint. Proc. from Clean. 2010 Int. Conf. Univ. Politec. Val. Museum Conserv. Inst.*, no. November 2010, pp. 51–58, 2013, [Online]. Available: https://repository.si.edu/bitstream/handle/10088/20489/11.Tumosa.SCMC3.Mecklenburg.Web.pdf?sequence=1&isAllowed=y.

[26] F. C. Izzo, M. Kratter, A. Nevin, and E. Zendri, ‘A Critical Review on the Analysis of Metal Soaps in Oil Paintings’, *ChemistryOpen*, vol. 10, no. 9, pp. 904–921, 2021, doi: 10.1002/open.202100166.

[27] J. D. J. Van Den Berg, K. J. Van Den Berg, and J. J. Boon, ‘Identification of non-cross-linked compounds in methanolic extracts of cured and aged linseed oil-based paint films using gas chromatography-mass spectrometry’, *J. Chromatogr. A*, vol. 950, no. 1–2, pp. 195–211, 2002, doi: 10.1016/S0021-9673(02)00049-3.

[28] A. Janas *et al.*, ‘Shrinkage and mechanical properties of drying oil paints’, *Herit. Sci.*,

vol. 10, no. 1, pp. 1–10, 2022, doi: 10.1186/s40494-022-00814-2.

[29] A. Sawicka *et al.*, 'Metal soap Efflorescence in Contemporary Oil Painting', *Issues Contemp. Oil Paint*, no. November 2015, 2014, doi: 10.1007/978-3-319-10100-2.

[30] I. Bonaduce *et al.*, 'New Insights into the Ageing of Linseed Oil Paint Binder: A Qualitative and Quantitative Analytical Study', *PLoS One*, vol. 7, no. 11, 2012, doi: 10.1371/journal.pone.0049333.

[31] S. M. P. Meneghetti, R. F. De Souza, A. L. Monteiro, and M. O. De Souza, 'Substitution of lead catalysts by zirconium in the oxidative polymerization of linseed oil', *Prog. Org. Coatings*, vol. 33, no. 3–4, pp. 219–224, 1998, doi: 10.1016/S0300-9440(98)00058-7.

[32] C. S. Tumosa and M. F. Mecklenburg, 'The influence of lead ions on the drying of oils', *Stud. Conserv.*, vol. 50, no. sup1, pp. 39–47, 2005, doi: 10.1179/sic.2005.50.supplement-1.39.

[33] T. A. Girard, M. Beispiel, and C. E. Bricker, 'The Mechanism of Cobalt Drier Action', *J. Am. Oil Chem.*, vol. 42, pp. 828–833, 1965.

[34] C. Stenberg, M. Svensson, and M. Johansson, 'A study of the drying of linseed oils with different fatty acid patterns using RTIR-spectroscopy and chemiluminescence (CL)', *Ind. Crops Prod.*, vol. 21, no. 2, pp. 263–272, 2005, doi: 10.1016/j.indcrop.2004.04.002.

[35] J. Mallégol, J. Lemaire, and J. Gardette, 'Drier influence on the curing of linseed oil', *Prog. Org. Coatings*, vol. 39, pp. 107–113, 2000.

[36] Z. Osawa, 'Role of metals and metal-deactivators in polymer degradation', *Polym. Degrad. Stab.*, vol. 20, no. 3–4, pp. 203–236, 1988, doi: 10.1016/0141-3910(88)90070-5.

[37] P. E. Marling, 'Accelerators and inhibitors of linseed oil drying'', *Can. Chem. Metall.*, vol. 11, pp. 63–66, 1927.

[38] M. F. Mecklenburg, C. S. Tumosa, and E. P. Vicenzi, 'The Influence of Pigments and Ion Migration on the Durability of Drying Oil and Alkyd Paints', *New Insights into Clean. Paint. Proc. from Clean. 2010 Int. Conf. Univ. Politec. Val. Museum Conserv. Inst.*, no. November 2010, pp. 59–67, 2013, [Online]. Available: https://repository.si.edu/bitstream/handle/10088/20490/12.Mecklenburg.SCMC3.Mecklenburg.Web.pdf?sequence=1&isAllowed=y.

[39] Juita, B. Z. Dlugogorski, E. M. Kennedy, and J. C. MacKie, 'Oxidation reactions and spontaneous ignition of linseed oil', *Proc. Combust. Inst.*, vol. 33, no. 2, pp. 2625–

2632, 2011, doi: 10.1016/j.proci.2010.06.096.

[40] L. L. Steele, 'Effect of Certain Metallic Soaps on the Drying of Raw Linseed Oil', *Ind. Eng. Chem.*, vol. 16, no. 9, pp. 957–959, 1924, doi: 10.1021/ie50177a043.

[41] J. Blockx, *Compendium. À l'usage des artistes peintres et des amateurs de tableaux*, Deuxiéme. Paris, 1892.

[42] G. Dorfles and A. Vettese, *Arti visive. Il Novecento: protagonisti e movimenti*. Bergamo: Atlas, 2004.

[43] L. de Viguerie, G. Ducouret, F. Lequeux, T. Moutard-Martin, and P. Walter, 'Historical evolution of oil painting media: A rheological study', *Comptes Rendus Phys.*, vol. 10, no. 7, pp. 612–621, 2009, doi: 10.1016/j.crhy.2009.08.006.

[44] J. Maroger, *À la recherce des secrets des grands peintres*. Dessain et Tolra, 1986.

[45] P. Vandenabeele, B. Wehling, L. Moens, H. Edwards, M. De Reu, and G. Van Hooydonk, 'Analysis with micro-Raman spectroscopy of natural organic binding media and varnishes used in art', *Anal. Chim. Acta*, vol. 407, no. 1–2, pp. 261–274, 2000, doi: 10.1016/S0003-2670(99)00827-2.

[46] R. Beninatto and O. De Lucchi, *Chimica organica per artisti e restauratori. Sostanze naturali*. CreateSpace, 2016.

[47] J. P. Helme and M. Rodde, 'Evolution des techniques de la peinture à l'huile', *OCL-Oléagineux, corps gras, lipides*, vol. 5, 1998.

[48] G. P. Lomazzo, *Della forma delle Muse*. Milano, 1591.

[49] L. Carlyle, *The Artist's Assistant: Oil Painting Instruction Manuals and Handbooks in Britain 1800-1900. With Reference to Selected Eighteenth-century Sources*. London: Archetype Publications, 2001.

[50] J. G. Vibert, *The science of painting*. London: P. Young, 1892.

[51] M. Geldof, I. D. van der Werf, and R. Haswell, 'The examination of Van Gogh's chrome yellow pigments in "Field with Irises near Arles" using quantitative SEM–WDX', *Herit. Sci.*, vol. 7, no. 1, pp. 1–11, 2019, doi: 10.1186/s40494-019-0341-3.

[52] G. P. DeWolf, 'Notes on Cultivated Labiates', *Baileya*, vol. 3, pp. 47–57, 1955.

[53] D. Herraiz-Peñalver, M. Á. Cases, F. Varela, P. Navarrete, R. Sánchez-Vioque, and J. Usano-Alemany, 'Chemical characterization of Lavandula latifolia Medik. Essential oil from Spanish wild populations', *Biochem. Syst. Ecol.*, vol. 46, pp. 59–68, 2013, doi: 10.1016/j.bse.2012.09.018.

[54] S. Paulraj, T. Selvamohan, and K. Kumaraswamy, 'GC-MS analysis of oil from Lavandula Latifolia and its repellent acitivy against mosquitos', *Int. J. Pharm. Sci.*

Res., vol. 12, no. 1, pp. 668–672, 2021, doi: 10.13040/IJPSR.0975-8232.12(1).668-72.

[55] C. Maltese, *Le tecniche artistiche*, Mursia. Milano, 1973.

[56] E. Barberis *et al.*, 'Leonardo's Donna Nuda unveiled', *J. Proteomics*, vol. 207, no. July, p. 103450, 2019, doi: 10.1016/j.jprot.2019.103450.

[57] M. Gnemmi, 'New insights into XXI century commercial artists oil paints. Morphological and molecular aspects during drying and curing', Ca' Foscari University of Venice, 2022.

[58] L. Fuster-López, F. C. Izzo, V. Damato, D. J. Yusà-Marco, and E. Zendri, 'An insight into the mechanical properties of selected commercial oil and alkyd paint films containing cobalt blue', *J. Cult. Herit.*, vol. 35, pp. 225–234, 2019, doi: 10.1016/j.culher.2018.12.007.

[59] S. Caravá, C. Roldán García, M. L. Vázquez de Agredos-Pascual, S. Murcia Mascarós, and F. C. Izzo, 'Investigation of modern oil paints through a physico-chemical integrated approach. Emblematic cases from Valencia, Spain', *Spectrochim. Acta - Part A Mol. Biomol. Spectrosc.*, vol. 240, pp. 30–32, 2020, doi: 10.1016/j.saa.2020.118633.

[60] I. Bonaduce and A. Andreotti, 'Py-GC/MS of Organic Paint Binders', *Org. Mass Spectrom. Art Archaeol.*, no. June 2016, pp. 303–326, 2009, doi: 10.1002/9780470741917.ch11.

[61] M. P. Colombini, F. Modugno, R. Fuoco, and A. Tognazzi, 'A GC-MS study on the deterioration of lipidic paint binders', *Microchem. J.*, vol. 73, no. 1–2, pp. 175–185, 2002, doi: 10.1016/S0026-265X(02)00062-0.

[62] L. Fuster-López *et al.*, 'Picasso's 1917 paint materials and their influence on the condition of four paintings', *SN Appl. Sci.*, vol. 2, no. 12, pp. 1–14, 2020, doi: 10.1007/s42452-020-03803-x.

[63] F. C. Izzo, A. Källbom, and A. Nevin, 'Multi-analytical assessment of bodied drying oil varnishes and their use as binders in armour paints', *Heritage*, vol. 4, no. 4, pp. 3402–3420, 2021, doi: 10.3390/heritage4040189.

[64] M. R. Derrick, D. Stulik, and J. M. Landry, *Infrared spectroscopy in Conservation Science*, vol. 1. Los Angeles: The Getty Conservation Institute, 1999.

[65] M. V. Russo and P. Avino, 'Characterization and Identification of Natural Terpenic Resins employed in " Madonna con Bambino e Angeli" by Antonello da Messina using Gas Chromatography-Mass Spectrometry', *Chem. Cent. J.*, vol. 6, no. 1, pp. 1–10, 2012, doi: 10.1186/1752-153X-6-59.

[66] A. Macchia *et al.*, 'Multi-Analytical Investigation of the Oil Painting "Il Venditore di Cerini" by Antonio Mancini and Definition of the Best Green Cleaning Treatment', *Sustain.*, vol. 14, no. 7, 2022, doi: 10.3390/su14073972.

[67] E. Possenti, C. Colombo, M. Realini, C. L. Song, and S. G. Kazarian, 'Insight into the effects of moisture and layer build-up on the formation of lead soaps using micro-ATR-FTIR spectroscopic imaging of complex painted stratigraphies', *Anal. Bioanal. Chem.*, vol. 413, no. 2, pp. 455–467, 2021, doi: 10.1007/s00216-020-03016-6.

[68] J. van der Weerd, A. van Loon, and J. J. Boon, 'FTIR studies of the effects of pigments on the aging of oil', *Stud. Conserv.*, vol. 50, no. 1, pp. 3–22, 2005, doi: 10.1179/sic.2005.50.1.3.

[69] L. Fuster-López, F. C. Izzo, M. Piovesan, D. J. Yusá-Marco, L. Sperni, and E. Zendri, 'Study of the chemical composition and the mechanical behaviour of 20th century commercial artists' oil paints containing manganese-based pigments', *Microchem. J.*, vol. 124, pp. 962–973, 2016, doi: 10.1016/j.microc.2015.08.023.

[70] L. Burgio and R. J. H. Clark, *Library of FT-Raman spectra of pigments, minerals, pigment media and varnishes, and supplement to existing library of Raman spectra of pigments with visible excitation*, vol. 57, no. 7. 2001.

[71] L. De Viguerie, P. A. Payard, E. Portero, P. Walter, and M. Cotte, 'The drying of linseed oil investigated by Fourier transform infrared spectroscopy: Historical recipes and influence of lead compounds', *Prog. Org. Coatings*, vol. 93, pp. 46–60, 2016, doi: 10.1016/j.porgcoat.2015.12.010.

[72] F. Rasti and G. Scott, 'The Effects of Some Common Pigments on the Photo-Oxidation of Linseed Oil-Based Paint Media', *Stud. Conserv.*, vol. 25, no. 4, pp. 145–156, 1980.

[73] M. Bacci and M. Picollo, 'Non-Destructive Spectroscopic Detection of Cobalt (II) in Paintings and Glass', *Stud. Conserv.*, vol. 41, no. 3, pp. 136–144, 1996.

[74] V. Otero *et al.*, 'Characterisation of metal carboxylates by Raman and infrared spectroscopy in works of art', *J. Raman Spectrosc.*, vol. 45, no. 11–12, pp. 1197–1206, 2014, doi: 10.1002/jrs.4520.

[75] K. Castro, M. Pérez-Alonso, M. D. Rodríguez-Laso, L. A. Fernández, and J. M. Madariaga, 'On-line FT-Raman and dispersive Raman spectra database of artists' materials (e-VISART database)', *Anal. Bioanal. Chem.*, vol. 382, no. 2, pp. 248–258, 2005, doi: 10.1007/s00216-005-3072-0.

[76] S. Akyuz, T. Akyuz, G. Emre, A. Gulec, and S. Basaran, 'Pigment analyses of a

portrait and paint box of Turkish artist Feyhaman Duran (1886-1970): The EDXRF, FT-IR and micro Raman spectroscopic studies', *Spectrochim. Acta - Part A Mol. Biomol. Spectrosc.*, vol. 89, pp. 74–81, 2012, doi: 10.1016/j.saa.2011.12.046.

[77] E. D. Teodor, S. C. Liţescu, A. Neacşu, G. Truică, and C. Albu, 'Analytical methods to differentiate Romanian amber and Baltic amber for archaeological applications', *Cent. Eur. J. Chem.*, vol. 7, no. 3, pp. 560–568, 2009, doi: 10.2478/s11532-009-0053-8.

[78] J. Park, E. Yun, H. Kang, J. Ahn, and G. Kim, 'IR and py/GC/MS examination of amber relics excavated from 6th century royal tomb in Korean Peninsula', *Spectrochim. Acta - Part A Mol. Biomol. Spectrosc.*, vol. 165, pp. 114–119, 2016, doi: 10.1016/j.saa.2016.04.015.

[79] I. D. van der Werf, A. Monno, D. Fico, G. Germinario, G. E. De Benedetto, and L. Sabbatini, 'A multi-analytical approach for the assessment of the provenience of geological amber: the collection of the Earth Sciences Museum of Bari (Italy)', *Environ. Sci. Pollut. Res.*, vol. 24, no. 3, pp. 2182–2196, 2017, doi: 10.1007/s11356-016-6963-z.

[80] S. Prati, G. Sciutto, R. Mazzeo, C. Torri, and D. Fabbri, 'Application of ATR-far-infrared spectroscopy to the analysis of natural resins', *Anal. Bioanal. Chem.*, vol. 399, no. 9, pp. 3081–3091, 2011, doi: 10.1007/s00216-010-4388-y.

[81] S. Vahur, A. Teearu, P. Peets, L. Joosu, and I. Leito, 'ATR-FT-IR spectral collection of conservation materials in the extended region of 4000-80 cm–1', *Anal. Bioanal. Chem.*, vol. 408, no. 13, pp. 3373–3379, 2016, doi: 10.1007/s00216-016-9411-5.

[82] Z. Chen, J. N. Hay, and M. J. Jenkins, 'FTIR spectroscopic analysis of poly(ethylene terephthalate) on crystallization', *Eur. Polym. J.*, vol. 48, no. 9, pp. 1586–1610, 2012, doi: 10.1016/j.eurpolymj.2012.06.006.

[83] 'Dali Salvador (1904-1989) - La tentation de Saint-Antoine 1946', in *Archives des Musées royaux des Beaux-Arts de Belgique*, p. Inv. 7223.

[84] M. Stols-Witlox, 'Grounds, 1400-1900', in *The Conservation of Easel Paintings*, 2nd ed., 2012, pp. 161–185.

[85] C. E. Brown, 'Pigments and fillers', *Mineralogy*, pp. 380–386, 1973, doi: 10.1007/0-387-30720-6_102.

[86] C. Daher, C. Paris, A. S. Le Hô, L. Bellot-Gurlet, and J. P. Échard, 'A joint use of Raman and infrared spectroscopies for the identification of natural organic media used in ancient varnishes', *J. Raman Spectrosc.*, vol. 41, no. 11, pp. 1204–1209, 2010, doi: 10.1002/jrs.2693.

[87] A. Barth, ‘Infrared spectroscopy of proteins’, *Biochim. Biophys. Acta - Bioenerg.*, vol. 1767, no. 9, pp. 1073–1101, 2007, doi: 10.1016/j.bbabio.2007.06.004.

[88] F. Adar, ‘Interpretation of Raman Spectrum of Proteins’, *Spectroscopy*, vol. 37, no. 2, pp. 9–13,25, 2022, [Online]. Available: https://cdn.sanity.io/files/0vv8moc6/spectroscopy/50f95b45661fba272b2f05636f37900654774673.pdf.

[89] Z. Tomić, P. Makreski, and B. Gajić, ‘Identification and spectra-structure determination of soil minerals: Raman study supported by IR spectroscopy and x-ray powder diffraction’, *J. Raman Spectrosc.*, vol. 41, no. 5, pp. 582–586, 2010, doi: 10.1002/jrs.2476.

[90] Y. Liu, A. Wang, and J. J. Freemen, ‘Raman, MIR and NIR spectroscopic study of calcium sulfates: gypsum, bassanite and anhydrite’, in *40th Lunar and Planetary Science Conference*, 2009.

[91] N. Prieto-Taboada, O. Gomez-Laserna, I. Martínez-Arkarazo, M. Á. Olazabal, and uan M. Madariaga, ‘Raman spectra of the different phases in the CaSO3 –H2O System’, *Anal. Chem.*, vol. 86, p. 10131−10137, 2014, doi: 10.1246/bcsj.55.738.

[92] N. Buzgar, A. Buzatu, and I. V. Sanislav, ‘The Raman study on certain sulfates’, *Analele Stiint. ale Univ. ‘ Al. I. Cuza’ din Iasi , Geol.*, vol. 55, no. 1, pp. 5–23, 2009, [Online]. Available: http://www.scopus.com/inward/record.url?eid=2-s2.0-84878729190&partnerID=tZOtx3y1%5Cnhttp://geology.uaic.ro/auig/article.php?id=26.

[93] A. Molea, V. Popescu, and N. A. Rowson, ‘The obtaining of nanostructured nitrogen doped titanium dioxide powders in presence of triethanolamine’, *Energy*, no. 2007, pp. 273–280, 2010.

[94] M. Ossman *et al.*, ‘Peanut shells and talc powder for removal of hexavalent chromium from aqueous solutions The direct bioorganic fuel cells View project Peanut shells and talc powder for removal of hexavalent chromium from aqueous solutions’, *Bulg. Chem. Commun.*, vol. 46, no. 3, pp. 629–639, 2014, [Online]. Available: https://www.researchgate.net/publication/269279024.

[95] A. Filopoulou, S. Vlachou, and S. C. Boyatzis, ‘Fatty acids and their metal salts: A review of their infrared spectra in light of their presence in cultural heritage’, *Molecules*, vol. 26, no. 19, 2021, doi: 10.3390/molecules26196005.

Appendix A

Table A1 Main infrared absorptions observed in ATR-FTIR spectra of Blockx oil paints and Dalí samples.

Peak (cm^{-1})	intensity	Vibrational mode	Assignement
3392	m	OH stretching	Fatty acid
3008	m	CH stretching	Fatty acid
2955	sh	CH_3 stretching	Fatty acid
2922	vs	CH_2 stretching	Fatty acid
2852	sh	CH_2 stretching	Fatty acid
1742	s	C=O stretching	Ester
1713		C=O stretching	Carboxylates
1653	m	C=C stretching	Ester
1623	sh	COO- bending	Fatty acid
1557		COO- asymmetric stretching	
1460	m	CH_3 asymmetric bending CH_2 scissoring	Fatty acid
1427	vw	Asymmetric stretching C-O	
1413	w	COO- stretching	Fatty acid
1378	m	CH_3 wagging	Fatty acid
1238	m	C-O asymmetric stretching	Ester
1160	m	C-O stretching	Ester
1098	m	C-O asymmetric stretching	Ester
972	m	Si-O stretching	Silicates
720	s	C=C-H bending	Fatty acid

Table A2 Retention time (min), molecular ion (m/z) and name of the main compounds observed in the chromatograms of Blockx oil paints.

Retention time (min)	Molecular ion (m/z)	Fatty acid ME 0 hours	Fatty acid ME 7 months
9.65	130	-	Pentanoic acid, 4-oxo ME
10.00	174	-	Octanoic acid, 8-hydroxy ME
10.19	89	Glycerol 89	Glycerol 89
10.40	162	Glycerol 162	Glycerol 162
10.48	172	Nonanoic acid, 9-oxo ME	Nonanoic acid, 9-oxo ME
10.61	202		Suberic acid diME
10.75	194	Phthalic acid diME	Phthalic acid diME
10.88	75	Glycerol 75	Glycerol 75
11.26	198	-	Methyl 10-oxo-8-decenoate
11.39	194	-	Terephtalic acid diME
11.54	200	-	Decanoic acid 9-oxo ME
11.87	216	Azelaic acid diME	Azelaic acid diME
13.05	230	-	Sebacic acid diME
13.90	241	Myristic acid ME	Myristic acid ME
14.38	360	-	Aleuritic acid, trimethyl ether ME

15.40	394	Glycerol 394	Glycerol 394
15.77	230	-	Octanedioic acid, 3,5-dimethyl diME
15.96	268	Palmitoleic acid ME	-
16.00	270	Palmitic acid ME	Palmitic acid ME
16.77	244	-	3-oxo-1,8-octanedicarboxylic acid diME
17.63	284	Palmitic acid, 14-methyl ME	-
17.63	292	Linoleic acid ME	Linoleic acid ME
17.69	296	Oleic acid ME	Oleic acid ME
17.91	298	Stearic acid ME	Stearic acid ME
18.19	294	Linolenic acid ME	Linolenic acid ME
18.81	312	Nonadecanoic acid ME	Nonadecanoic acid ME
19.29	312	-	Oxiraneoctanoic acid, 3-octyl ME
19.49	312	-	Stearic acid, 9-oxo ME
19.55	326	Eicosanoic acid ME	-
19.67	314	-	Stearic acid, 12-hydroxy ME
19.80	134	Glycerol main	Glycerol main
20.38	330	-	Octadecenoic acid, 9,10-dihdroxy ME
21.29	354	-	Behenic acid ME